Impact Investigation of Source Correlation on IDMA-based Multi-User Detection

Jiajie Xue

School of Information Science,
Japan Advanced Institute of Science and Technology,
December, 2016

Master's Thesis

Impact Investigation of Source Correlation on IDMA-based Multi-User Detection

1410206 Jiajie Xue

Supervisor : Tadashi Matsumoto
Main Examiner : Tadashi Matsumoto
Examiners : Brian M. Kurkoski
Kiyofumi Tanaka

School of Information Science,
Japan Advanced Institute of Science and Technology

November, 2016

I certify that I have prepared this Master's Thesis by myself without any inadmissible outside help.

Jiajie Xue
JAIST, 17 November, 2016

Author : _____

Date : _____

Supervisor : _____

Vice Supervisor : _____

Minor Research Supervisor : _____

Abstract

The primary objective of this thesis is to identify the impact of the source correlation on multi-user detection (MUD). The necessary condition of correlated sources transmitted over multiple access channel (MAC) is still an open question in Network Information Theory, hence instead of pursuing pure information theoretic approach, the empirical methods are taken in this thesis. Since the interleave division multiple access (IDMA) has excellent spectral efficiency, bit-interleaved coded modulation using iterative decoding (BICM-ID) based IDMA with soft successive interference cancellation (SSIC) is chosen as the multiple access scheme. Bit-flipping model and a very simple irregular repetition (IrR) code are exploited as the correlated sources generation method and the channel code in this thesis, respectively.

First of all, this thesis investigates the case that channel decoding for different users are performed independently. The system model of BICM-ID based IDMA with SSIC for investigation is presented under additive white Gaussian noise (AWGN) channel assumption based on fundamental principles and techniques. A frequency domain soft cancellation minimum mean square error (FD-SC-MMSE) turbo equalizer is jointly utilized in the system model to eliminate inter-symbol interference (ISI) in frequency selective fading channel. Simulation results show that, with independent decoding performed at the receiver, the source correlation does not make any impact on system bit error rate (BER) and/or frame error rate (FER) performance in the presented IDMA system.

This thesis then investigates the joint decoding process which aims to utilize the source correlation at the receiver to improve system BER and/or FER performance. By using extrinsic information transfer chart (EXIT chart), it is shown that, with relatively high source correlation, joint decoder can significantly increase the *extrinsic* log likelihood ratio (LLR) to help decoding process. Simulation results show the same conclusion that the system performance can be significantly improved with relatively high source correlation. Moreover, in the frequency selective fading channel, if sources are not fully correlated, the diversity order does not increase, only a parallel shift of FER curves is observed. However, with fully correlated source, the diversity order increases to twice.

Furthermore, a trade-off between rate-sum and performance gain is then analysed through Slepian-Wolf (S-W) and MAC rate region based on the sufficient condition of the problem of correlated sources transmitted over MAC. This trade-

off analysis indicates that with limited physical resources the excellent transmission efficiency and excellent reliability can not be achieved at the same time. Particularly, this analysis result can also help us to flexibly allocate power and transmission rate in cooperative communication systems.

Keywords: source correlation, S-W region, MAC, IDMA, BICM-ID, AWGN channel, frequency selective fading channel, FD-SC-MMSE, joint decoder, IrR, rate-sum / performance gain trade-off

Acknowledgments

First of all, I would like to thank my supervisor Prof. Tadashi Matsumoto (Tad), who gives me continuous guidance and encouragement of my study, research and job-hunting in Japan. He is my supervisor in research life, and also like a mentor and friend of me in daily life. I learned a lot from Tad, not only academic knowledge, but also attitude of facing challenges and will benefit me through my life time.

I would like to thank professors and colleagues who help me a lot in my life in JAIST. Thanks to my co-supervisor Prof. Brian Kurkoski, who gave me a lot valuable comments of my research in these two years. Thanks to Prof. Kiyofumi Tanaka for his evaluation and comments of my research. Thanks to Prof. Jianwu Dang for his supervise of my minor research, which is a very interesting topic and I learned a lot from him. Thanks to Dr. Meng Cheng, who gave me a guidance of life in JAIST when I just arrived at JAIST. Thanks to Dr. Xin He, who helped me on my research and my programming skills. Thanks to Dr. Shen Qian, who helped me on my abroad daily life and encouraged my a lot during my job-hunting. My sincere thanks also goes to Ade, Alan, Anwar, Erick, Fan, Hasan, Javier, Reza, Ricardo, Ryota, Shofi, Thanh and all the university stuffs. All of you supported me on my research and life in Japan during these two years, and we made many memories that I will keep them in my heart forever.

Last but not least, I want to thank my family, who have been keeping supporting and encouraging on me for my study abroad and in my life time.

Table of Contents

Acknowledgments **v**

List of Figures **viii**

List of Tables **ix**

Abbreviations **x**

Notations **xii**

Chapter 1
Introduction **1**
1.1 Background 1
1.2 Summary of Thesis 3
1.3 Thesis Outline 3

Chapter 2
Preliminaries **5**
2.1 IDMA Principle 5
2.2 Channel Model 8
2.2.1 AWGN Channel 8
2.2.2 AWGN Channel Capacity 9
2.2.3 Fading Channel 9
2.2.4 Outage Probability 11
2.2.5 Multiple Access Channel 11
2.3 Correlated Sources 12
2.4 Coding and Modulation Schemes 14
2.4.1 BICM-ID Principle 15
2.4.2 Doped Accumulator 17
2.4.3 QPSK Demapper 18
2.4.4 EXIT Chart Analysis 18
2.4.5 Coding and Decoding scheme 20
2.5 Summary 21

Chapter 3
Impact Investigation of Source Correlation **22**
3.1 Introduction . . . 22
3.2 System Model . . . 23
3.2.1 Transmission Scheme . . . 23
3.2.2 MUD and Decoding Schemes . . . 25
3.3 Joint Turbo Equalizaion and MUD scheme . . . 27
3.3.1 Channel Matrix . . . 28
3.3.2 Joint FD-SC-MMSE Equalizer and Demapper . . . 29
3.3.3 MUD and Decoding Scheme . . . 32
3.4 Numerical Reaults . . . 32
3.4.1 BER Performance in AWGN Channel . . . 33
3.4.2 FER Performance in Frequency Seletive Fading Channel . . . 37
3.5 Summary . . . 41

Chapter 4
Impact Investigation on Source Correlation with Joint Decoder **42**
4.1 Introduction . . . 42
4.2 System Model . . . 43
4.2.1 Joint Decoding scheme . . . 43
4.2.2 Iteration Scheme . . . 46
4.3 Numerical Results . . . 46
4.3.1 AWGN channel . . . 48
4.3.2 Frequency selective fading channel . . . 48
4.4 Rate-sum / Performance Gain Trade-off . . . 53
4.5 Summary . . . 56

Chapter 5
Conclusions and Future Work **57**
5.1 Conclusions . . . 57
5.2 Future Work . . . 58

List of Figures

2.1 Conventional IDMA System Model 7
2.2 Rate Region of Multiple Access Channel 12
2.3 Achievable Region based on Slepian-Wolf Theorem 13
2.4 Example of MAC Region and S-W Region Intersection Analysis . . 14
2.5 BIDM-ID Transmitter and Receiver Model 15
2.6 QPSK Constellations with Gray and Non-Gray Mmapping 16
2.7 Structure of Doped Accumulator 17
2.8 EXIT Chart of Demapper and Decoder at $SNR = 2dB$ 19

3.1 IDMA-based MUD System Model 24
3.2 Structure of Joint FD-SC-MMSE Equalizer and Demapper 30
3.3 BER performance for the 1st user in AWGN channel 35
3.4 BER performance for the 2nd user in AWGN channel 36
3.5 FER performance for the 1st user in frequency selective fading channel 39
3.6 FER performance for the 2nd user in frequency selective fading channel 40

4.1 IDMA-based MUD System Model with Joint Decoder 44
4.2 3D EXIT chart for fc function, demapper and IrR decoder with $SNR = 0dB$, $\rho = 0.25$ and 0.75 47
4.3 BER performance for the 1st user using joint decoder in AWGN channel 49
4.4 BER performance for the 2nd user using joint decoder in AWGN channel 50
4.5 FER performance for the 1st user using joint decoder in frequency selective fading channel 51
4.6 FER performance for the 2nd userusing joint decoder in frequency selective fading channel 52
4.7 Rate-sum/ performance gain trade-off analysis with $(E_{s1}+E_{s2})/\sigma_n^2 = 0.9103dB$ and $E_{s1}/E_{s2} = 1.5$ 55

List of Tables

3.1 Parameters and algorithms for simulation in AWGN channel 34
3.2 Parameters and algorithms for simulation in frequency selective fading channel 38

Abbreviations

8PSK	8 Phase-Shift Keying
AWGN	Additive White Gaussian Noise
BCJR	Bahl, Cocke, Jelinek and Raviv
BER	Bit Error Rate
BICM-ID	Bit-Interleaved Coded Modulation Using Iterative Decoding
CDMA	Code Division Multiple Access
CP	Cyclic prefix
DACC	Doped Accumulator
DFT	Discrete Fourier Transform
EXIT chart	EXtrinsic Information Transfer Chart
FDMA	Frequency Division Multiple Access
FD-SC-MMSE	Frequency Domain Soft Cancellation Minimum Mean Square Error
FER	Frame Error Rate
IDMA	Interleave Division Multiple Access
IrR code	Irregular Repetition Code
ISI	Inter-Symbol Interference
LLR	Log Likelihood Ratio
MAC	Multiple Access Channel
MAI	Multiple Access Interference
MAP	Maximum *a posteriori*

MLSE	Maximum Likelihood Sequence Estimation
MUD	Multi-user Detection
NOMA	Non-orthogonal Multiple Access
PDF	Probability Density Function
QoS	Quality of Service
QPSK	Quadrature Phase-Shift Keying
RSC code	Recursive Systematic Convolutional Code
SINR	Signal-to-Interference-plus-Noise Ratio
SNR	Signal-to-Noise Ratio
SSIC	Soft Successive Interference Cancellation
S-W region	Slepian-Wolf Region
TDMA	Time Division Multiple Access
V2V	Vehicle to Vehicle
WSN	Wireless Sensor Networks

Notations

p_e	Bit-flipping Probability
ρ	Source correlation
K	Number of Users
k	User Index
N_b	Length of Information bit Sequence
N_s	Length of Transmitted Symbol Sequence
E_b	Energy of per Information bit
E_s	Energy of per Transmitted Symbol
P_k	Transmission Power of k-th User
u	Information Sequence
$\hat{u}$	Estimated Information Sequence
x	Transmitted Signal
y	Received Signal
n	Gaussian Noise
ζ_k	Interference Experienced by k-th user
h	Channel Impulse Response
L	Channel Length
$\mathbf{H}$	Channel Matrix
$\mathbf{H}^c$	Circulant Channel Matrix
$\hat{x}$	Estimated Soft Symbol

$\hat{y}$	Symbol Sequence after SSIC
$\tilde{y}$	Residual of y
σ_n^2	Variance of Gaussian Noise
σ_k^2	Variance of k-th User
$\sigma_{k,\zeta}^2$	Variance of Interference Experienced by k-th User
$\mathbf{F}$	Normalized DFT Matrix
z_k	Equalized Symbol Sequence
μ_z	First Moment of z_k
σ_k^2	Second Moment of z_k
$\mathbf{I}_{a,Dem}^c$	*a priori* Mutual Information of Demapper Coded Bits Input
$\mathbf{I}_{e,Dem}^c$	*extrinsic* Mutual Information of Demapper Coded Bits Output
$\mathbf{I}_{a,Dec}^c$	*a priori* Mutual Information of Decoder Coded Bits Input
$\mathbf{I}_{e,Dec}^c$	*extrinsic* Mutual Information of Decoder Coded Bits Output
$\mathbf{I}_{a,Dec}^u$	*a priori* Mutual Information of Decoder Systematic Bits Input
$\mathbf{I}_{e,Dec}^u$	*extrinsic* Mutual Information of Decoder Systematic Bits Output
$L_{k,e,ESE}$	ESE Function *extrinsic* LLR of k-th user
$L_{k,p,Dec}^c$	Decoder *a posteriori* LLR of Coded Bits of k-th user
$L_{k,a,Dec}^c$	Decoder *a priori* LLR of Coded Bits of k-th user
$L_{k,a,Dec}^u$	Decoder *a priori* LLR of Systematic Bits of k-th user
$L_{k,e,Dec}^c$	Decoder *extrinsic* LLR of Coded Bits of k-th user
$L_{k,e,Dec}^u$	Decoder *extrinsic* LLR of Systematic Bits of k-th user
$L_{k,a,Dem}$	Demapper *a priori* LLR of k-th user
$L_{k,e,Dem}$	Demapper *extrinsic* LLR of k-th user
$L_{k,a,Soft}$	Soft Symbol Generator *a priori* LLR of k-th user

Chapter 1

Introduction

1.1 Background

In modern telecommunication systems, especially in wireless communication systems, resources division multiple access technique, which is also known as xDMA, is an indispensable part in systems. x can be time, with which x= T, frequency, x= F, space, x= S, and/or other resources. Since NOMA techniques such as CDMA and IDMA, outperform orthogonal multiple access techniques such as TDMA and FDMA, in term of spectral efficiency [1], NOMA techniques have been recognised as being important in broadband wireless communications, including mobile communications. An in-depth comparative study between IDMA and CDMA is provided in [2]. Since IDMA achieves an excellent spectral efficiency, because of its potential capability of multi-user detection, IDMA is chosen as the multiple access technique in this research. The concept of IDMA is introduced in [2, 3] and [4]. Nowadays, many applications based on IDMA have been proposed. IDMA is also considered as one of candidates for the next generation wireless communications systems.

In cooperative communications, such as WSN or V2V network, source information transmitted from different nodes are very likely correlated. Therefore, it is natural to investigate if the source correlation makes any impact on system performance of IDMA-based MUD. Furthermore, it is also a interesting topic to identify if the decoders can utilize the source correlation to help decoding process in order to achieve better system performance. If it is possible to improve the system performance by utilizing the source correlation, better spectral efficiency can further be improved.

In this section, we provide the historical background of this thesis, as well as the related fundamental techniques. The background and history of this thesis is as following:

Turbo Code It is a Shannon capacity achieving code and is proposed in [5]. Based on the turbo code, the iterative decoding technique is developed, by which a significant improvement of decoding performance can be achieved.

BICM-ID The basic BICM principle is first proposed by Zehavi in [6], with a purpose of increasing the diversity order of the trellis-coded-modulation [7]. At the receiver side, in order to improve decoding performance, Li and Ritcey apply the iterative decoding process, which is provided in [8] and is called BICM-ID. In turbo code, the decoding function of two component codes are complicated. However, with the BICM-ID principle, one component code can be replaced by the modulator and the channel code can not necessary be a very strong code, therefore, the decoding complexity can be significant reduced without performance loss.

BICM-ID with Extended Mapping This topic is an application of BICM-ID with optimized mapping scheme which is proposed in [9]. With the extended mapping, the EXIT chart for demapper can be reshaped to achieve better convergence property.

BICM-ID based IDMA This topic combines principles of BICM-ID and IDMA which are naturally suitable to each other. With the system proposed in [10] and [11], a near capacity performance can be achieved.

BICM-ID based IDMA with SSIC This topic includes the MUD part in IDMA system and its convergence properties in AWGN channel and frequency selective fading channel [12] and [13].

Impact of Source Correlation on IDMA-based MUD This topic is referred to this thesis. In this thesis, the impact caused by source correlation is first investigated. Then by utilizing the source correlation, it is shown that the system can achieve better performance than independent decoding case.

1.2 Summary of Thesis

The primary objective of this research is to identify the impact of the source correlation on MUD. This topic includes some problems not yet solved by Network Information Theory, and hence, instead of pursuing pure information theoretic approach, we take empirical methods where we reveal the behavioural properties of IDMA with SSIC.

In this thesis, it can be concluded that, in the IDMA system, the source correlation does not make any impact on MUD and decoding performance, if the independent decoding process is applied for each user, under the AWGN channel and the frequency selective fading channel assumptions. Furthermore, by utilizing the source correlation in the joint decoding process at the receiver, the IDMA system can achieve better performance when sources have higher correlation. Moreover, the rate-sum / performance gain trade-off is analysed through S-W region and MAC region analysis. This trade-off is useful for analysing the achievable rate region. It can also help to allocate and optimize the powers and/or transmission rates to achieve efficient utilization of physical resources depending on the QoS requirement of applications.

1.3 Thesis Outline

This thesis is organized into 5 chapters.

In Chapter 1, the background and motivation of this research are introduced, followed by the summary of this research and the outline of this thesis.

In Chapter 2, several fundamental concepts and earlier works are introduced. First of all, the IDMA principle is introduced. Then, the mathematical model of AWGN channel and frequency selective fading channel are provided. The problem of correlated sources transmitted over MAC is also introduced in Chapter 2 as well. After that, techniques related to coding and modulation are introduced.

In Chapter 3, impact investigation of source correlation on IDMA-based MUD with independent decoding is provided. The system model with related techniques used in the AWGN channels are first provided. Under the frequency selective fading channel assumption, to eliminate the ISI, a FD-SC-MMSE turbo equalizer is used, where the system model is modified for frequency selective fading channel. Then, the numerical results based on computer simulation are provided

under AWGN channel and frequency selective fading channel assumptions with independent decoding, followed by discussions of the simulation results.

Chapter 4 is the most important chapter of this thesis, where the impact investigation of source correlation on IDMA-based MUD with joint decoding is provided. In this chapter, the structure and properties of the joint decoder is first provided with corresponding EXIT analysis. Then a modified iteration scheme is discussed in order to eliminate the total number of iteration times. Numerical results are provided using the same parameter settings as in Chapter 3. After that, a trade-off between rate-sum and system performance is discussed by comparing the rate-sum and system performance with different source correlation.

In Chapter 5, the summary and topics of the future works are provided.

Chapter 2

Preliminaries

In this chapter, some basic principles and concepts in this research are provided. Also some earlier work and State-of-the-Art techniques involved in this research are introduced. First of all, basic principle of IDMA, which is the core part of this research, is briefly introduced. Then, mathematical models of channels including AWGN channel, frequency selective fading channel and multiple access channel are introduced. After that, the problem of correlated sources transmitted over MAC is introduced with some related earlier works. Finally, details of some techniques in this research including signalling, modulation, channel coding and decoding schemes are introduced.

2.1 IDMA Principle

As discussed in Chapter 1, IDMA is chosen as the candidate of the multiple access scheme in this thesis due to the excellent spectral efficiency.

The concept of IDMA is introduced in [2, 3] and [4]. Instead of using spreading codes for user separation as in CDMA systems, IDMA allocates random and unique interleaver to each user for user separation. With the iterative detection, compared with one-shot detection in CDMA, system performance of IDMA systems can achieve the turbo gain during iteration. In IDMA system, receiver performs joint detection and channel decoding iteratively to separate users and decode informations. The IDMA has exhibited various advantages in research, part of which are introduced in [1] and [3]. IDMA has been proposed for many applications and also considered as one of candidates for the next generation of wireless communi-

cation systems.

The conventional system model of IDMA is shown in Fig. 2.1. At the transmitter side, each user has its own interleaver which is different user by user. Before modulation, coded sequences will be first sent to user-specified interleavers which are also known at the receiver side.

Under the assumption of K simultaneous users, as shown in Fig. 2.1, information sequence u_k ,where $k \in \{1, 2, \cdots, K\}$, is first encoded by a channel encoder to generate coded sequence c_k. Then, c_k is per-mutated by its own interleaver Π_k to generate an interleaved version of c_k. After that, the interleaved version of c_k is mapped to signal symbol x_k by using a specified mapping rule. Finally, mapped signal x_k is sent to receiver over MAC.

At the receiver, iterative joint detection and decoding is performed to recover the original information sequence u_k. The MAC output y received by antenna(s) can be expressed as

$$y_m = \sum_{k=1}^{K} x_{k,m} + n_m, \tag{2.1}$$

where m and n_m denote symbol index and additive white Gaussian noise component with variance σ_n^2, respectively. The MAC output can also be reformed into

$$y_m = x_{k,m} + \zeta_{k,m}, \tag{2.2}$$

where ζ is called multiple access interference which is the summation of Gaussian noise and all the other users' signal, and can be expressed as

$$\zeta_{k,m} = \sum_{g=1, g\neq k}^{K} x_{g,m} + n_m. \tag{2.3}$$

The elementary signal estimator function is first activated to eliminate interference of MAC output for each user. For the k-th user, ESE output *extrinsic* LLR $L_{k,e,ESE}$, defined as $L_{k,e,ESE} = p(x = 1|y)/p(x = 0|y)$, is sent to a de-interleaver, which performs the inverse permutation of the *extrinsic* LLR, corresponding to the one used in the transmitter. Then channel decoding is performed. After that, based on turbo principle, *extrinsic* informations are exchanged between ESE function and channel decoder iteratively to estimate the original information.

The core principle of IDMA system is that each user uses a unique interleaver

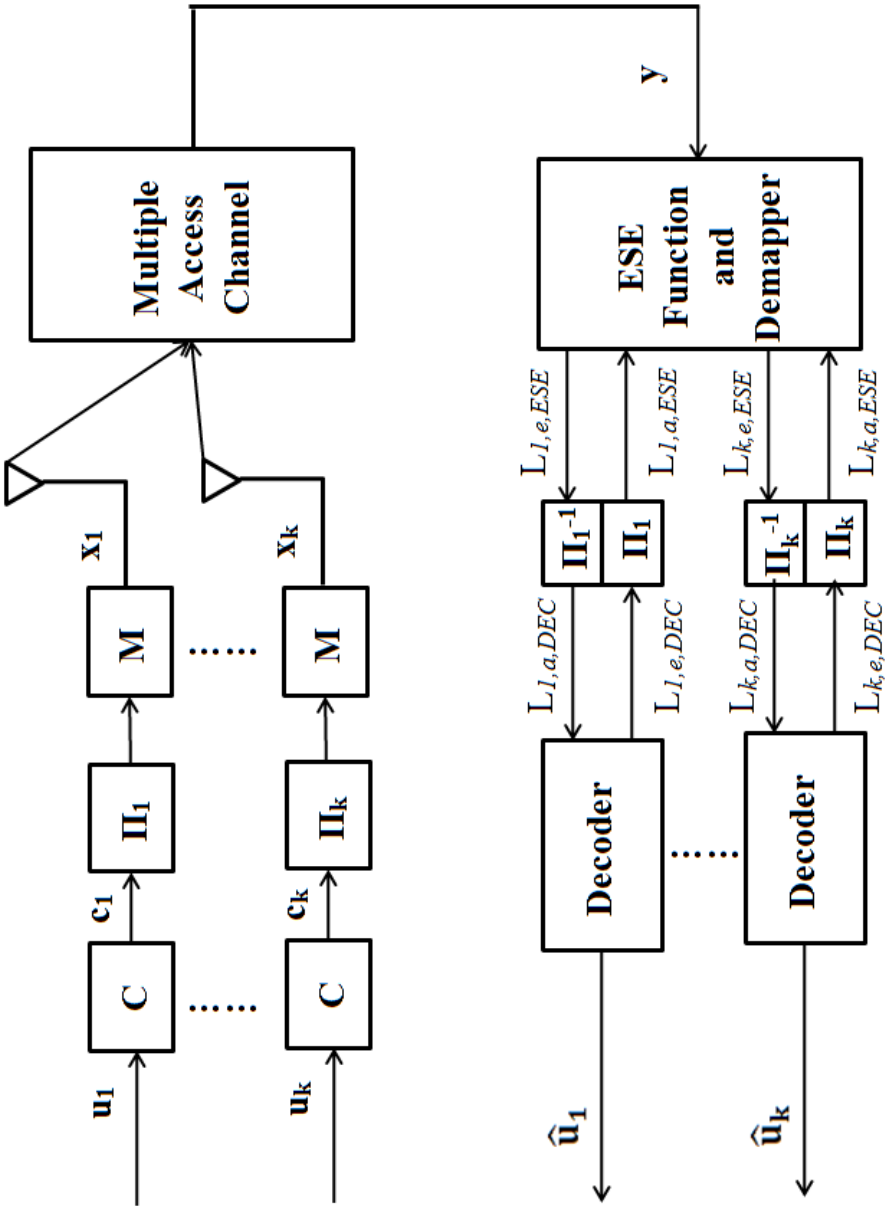

Figure 2.1. Conventional IDMA System Model

Π_k to the user identification. Interleavers in IDMA system are generated randomly and independently to guarantee that the interleaved sequences are statistically independent among the users. According to central limit theorem, summation of a series of independent variables can be approximated by a Gaussian random variable. Therefore, interference ζ_k in Equ. (2.2) is equivalent to an additive Gaussian noise, which is a very useful assumption in this research.

In this section, we only discuss the basic principle and advantages of IDMA system. Further details of IDMA system model used in this research will be discussed in the next chapter.

2.2 Channel Model

In telecommunication systems, the physical medium between transmitter and receiver is called channel. There are various types of physical media. To simplify analysis in research, it is quite common way that only mathematical properties are considered to describe and classify channels. In this research, AWGN channel, frequency selective fading channel and MAC are used as channel models for investigating impact of source correlation in the IDMA systems. In this section, mathematical expressions are first provided for each channel model. Then, capacity, outage probability and rate region in the AWGN channel, frequency selective fading channel and MAC, respectively, are given.

2.2.1 AWGN Channel

Additive White Gaussian Noise channel, which is usually abbreviated by AWGN channel, is one of basic and practical channel models. The mathematical description of AWGN channel is

$$\mathbf{y} = \mathbf{x} + \mathbf{n}, \tag{2.4}$$

where received signal $\mathbf{y}$ is equal to transmitted signal $\mathbf{x}$ added by a white Gaussian noise $\mathbf{n}$. The noise $\mathbf{n}$ distributes over independent and identically distributed (i.i.d.) random variables following two-dimensional Gaussian distribution with $\mu = 0$ and $\sigma_n^2 = N_0/4$ per-dimension, where N_0 is spectral density of noise.

AWGN channel model doesn't consider fading, caused by multipath propagation or shadowing, and other physical phenomenons except Gaussian noise. How-

ever, it provides a simple and useful way to investigate basic system performance before taking into account of other physical phenomenons.

2.2.2 AWGN Channel Capacity

Channel capacity is the upper bound on the rate at which information can be transmitted with arbitrary low error over a communication channel, and can be defined as

$$C = \max_{p(x)} \ \mathrm{I}(\mathbf{X};\ \mathbf{Y}), \tag{2.5}$$

where the channel capacity C is equal to the maximum mutual information between channel input and output over input distribution $p(x)$.

The theorem of noisy channel capacity is first proposed on [14] by Claude E. Shannon at 1948. According to Shannon's work, the channel capacity can be further expressed as

$$C = \mathrm{B} \cdot \log_2\ (1 + \gamma), \tag{2.6}$$

where B and γ are the bandwidth and the instantaneous SNR, respectively. A Gaussian codebook with rate $\mathbf{R} \leq \mathbf{C}$ can be designed to achieve arbitrary low error in transmission, when γ is given.

In this research, complex Gaussian channel is used where the noise is two dimensionally distributed with $\sigma_n^2 = N_0/2$. In this case, channel capacity can be expressed as

$$C = \log_2\ \left(1 + \frac{E_c}{N_0}\right), \tag{2.7}$$

where E_c and $E_c\,/\,N_0$ are average energy of coded symbol and received SNR, respectively, if the Nyquist bandwidth B of receiver filter is equal to the inverse of the symbol duration.

2.2.3 Fading Channel

In Section 2.2.1 and 2.2.2, mathematical model of AWGN channel and its capacity are introduced. The AWGN channel model ignores all the other physical phenomenons for the simplicity. However, in this section, fading and its frequency selectivity is discussed.

Flat fading channel

In wireless communications, received signal power varies randomly over distance or time as a result of shadowing and/or multipath fading, which is usually modelled as a random process. In mathematical analysis, Jakes' model is widely used to represent Rayleigh fading channel. Its details are provided in [15]. We simply utilize

$$\mathbf{y} = h \cdot \mathbf{x} + \mathbf{n}, \tag{2.8}$$

where h is called channel gain and is a complex random variable. Each dimension of h follows the Gaussian distribution with $\mu = 0$ and $\sigma^2 = 1/2$. The expected value of channel energy $E[|h|^2]$ is usually normalized to 1.

Frequency selective fading channel

In modern wireless communications, broadband transmission is widely used due to the requirement of transmission speed. However, in this case, received signal usually suffers from multipath propagation, which results in signal components reaching destination at different times due to different propogation lengths. This phenomenon is usually non-negligible in the broadband transmission because the bit period is shorter than the channel's delay spread [7]. The mathematical description of multipath channel is

$$\mathbf{y} = \mathbf{H} \cdot \mathbf{x} + \mathbf{n}, \tag{2.9}$$

where $\mathbf{H}$ is channel matrix defined as

$$\mathbf{H} = \begin{pmatrix} h_0 & & & \mathbf{O} \\ h_1 & h_0 & & \\ \vdots & h_1 & \ddots & \\ h_{L-1} & \vdots & \ddots & h_0 \\ & h_{L-1} & \ddots & h_1 \\ \vdots & \vdots & \vdots & \vdots \\ \mathbf{O} & & & h_{L-1} \end{pmatrix}, \tag{2.10}$$

where h_l, $l \in [0, L-1]$, is the channel gain for each path and each dimension follows the Gaussian distribution with $\mu = 0$ and $\sigma^2 = 1/2L$. Note that the expect

value of channel energy is also normalized as

$$E\left[\sum_{l=0}^{L-1} |h_l|^2\right] = 1. \tag{2.11}$$

It should be noticed that multipath propagation may result in frequency selectivity on the received signal. For a two-path channel whose impulse response is $h = [a, b]$ (assume $a, b \geq 0$), Fourier transform of h can be expressed as

$$\mathrm{H}(j\omega) = a + b \cdot e^{-j\omega t_0}, \tag{2.12}$$

where t_0 is channel delay. With angle frequency point $\omega = \pi/t_0$, Equ. (2.12) takes its minimum value $a - b$ which sometime results in very deep fade at the receiver.

Although impulse response of a fading channel usually varies with time, in this research, we assume that impulse response doesn't change within one transmission block, but vary with block by block, which is referred to block fading channel model.

2.2.4 Outage Probability

In AWGN channel, the probability of symbol error depends on the received SNR. However, in fading channel, since the channel impulse response varies with time, received SNR is also changing with the time. Therefore, outage probability is defined as a performance criteria for fading channel. The outage probability is defined as

$$P_{out} = P(\gamma_s < \gamma_0) = \int_0^{\gamma_0} p_{\gamma_s}(\gamma)\, d\gamma, \tag{2.13}$$

where γ_0 typically specifies the minimum SNR required for acceptable performance and γ_s is instantaneous SNR [16]. $p_{\gamma_s}(\gamma)$ is the PDF of γ_s.

2.2.5 Multiple Access Channel

Another channel model used in this research is multiple access channel in which two or more users send informations to a common receiver. As mentioned in Section 2.1, NOMA is considered in this research. The output of MAC can be expressed

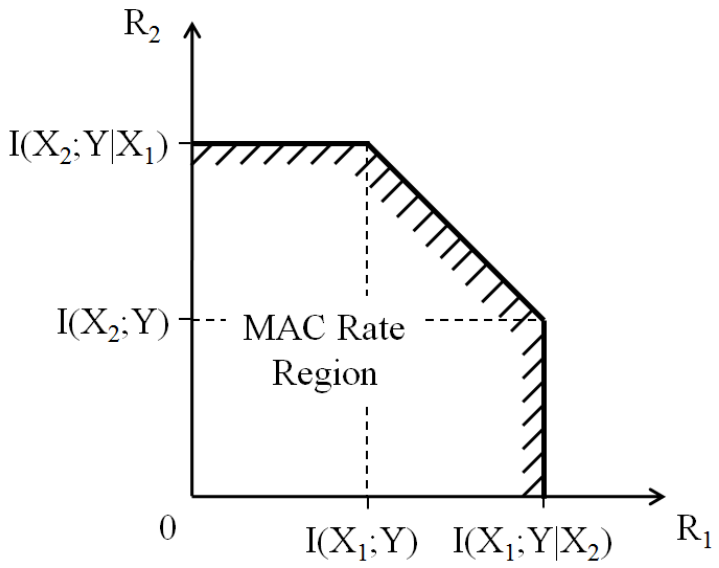

Figure 2.2. Rate Region of Multiple Access Channel

as

$$\mathbf{y} = \sum_{k=1}^{K} \mathbf{x}_k + \mathbf{n}, \tag{2.14}$$

where K donates the number of users. For a two users MAC, the rate region is the closure of the set of achievable (R_1, R_2) rate pairs, which satisfies

$$\begin{cases} R_1 & \leq & \mathbf{I}(X_1\,;\,Y\,|\,X_2) \\ R_2 & \leq & \mathbf{I}(X_2\,;\,Y\,|\,X_1) \\ R_1 + R_2 & \leq & \mathbf{I}(X_1,\,X_2\,;\,Y) \end{cases}, \tag{2.15}$$

and is illustrated in Fig. 2.15 [17].

2.3 Correlated Sources

Another key word of this research is correlated sources which are very common in coorprative communications and wireless sensor networks. A theoretical bound of coding two lossless compressed correlated sources was provided by Slepian and Wolf in 1973 [18]. Correlated sources can be losslessly compressed within the rate

region satisfying Equ. (2.16) which is illustrated in Fig. 2.3.

$$\begin{cases} R_1 \geq H(X_1 \,|\, X_2) \\ R_2 \geq H(X_2 \,|\, X_1) \\ R_1 + R_2 \geq H(X_1, X_2) \end{cases} . \tag{2.16}$$

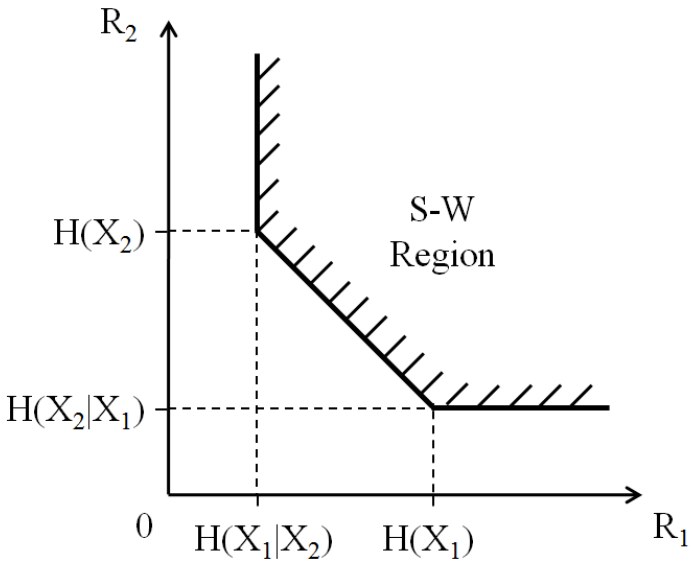

Figure 2.3. Achievable Region based on Slepian-Wolf Theorem

In this research, we consider two correlated sources which are transmitted over a non-orthogonal MAC. Therefore, both MAC region and Slepian-Wolf region (S-W region) should be considered. About this problem, Cover, El Gamal and Salehi proven the sufficient condition of lossless communication of a pair of correlated sources using joint source-channel coding over a discrete MAC in 1980 [19]. However, the necessary condition of this problem is still an open problem [20]. The outage probability of correlated sources transmitted over orthogonal block Rayleigh fading channel was derived in [21]. Correlated sources transmitted over one-path fading channel was investigated in [22]. The sufficient condition for fading MAC with given distortions and optimal power allocation was deived in [23]. Outage probability in non-orthogonal fading MAC based on the sufficient condition was derived at [24]. Also, correlated sources transmitted over multi-path fading MAC with two receive antennas and joint decoding were proposed in [25] and [26].

Based on the result in [19], the sufficient condition can be obtained by combining Equ. (2.15) and Equ. (2.16),

$$\begin{cases} H(X_1 \,|\, X_2) & \leq & \mathbf{I}(X_1 \,;\, Y \,|\, X_2) \\ H(X_2 \,|\, X_1) & \leq & \mathbf{I}(X_2 \,;\, Y \,|\, X_1) \\ H(X_1,\, X_2) & \leq & \mathbf{I}(X_1,\, X_2 \,;\, Y) \end{cases} . \tag{2.17}$$

Equ. (2.17) indicates that the transmission is succeeded, if MAC region and S-W region intersect with each other, otherwise transmission is failed, as shown in Fig. 2.4 [24].

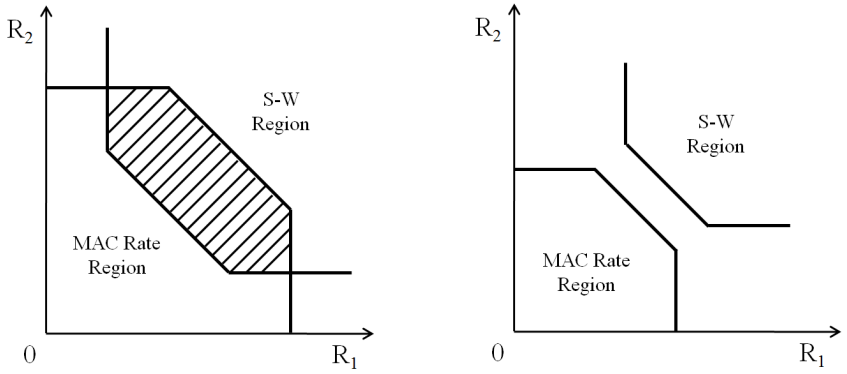

(a) Transmission success (b) Transmission fail

Figure 2.4. Example of MAC Region and S-W Region Intersection Analysis

Since the necessary condition of this problem is still an open problem, in this research, only empirical methods are used to investigate impact of source correlation on IDMA-based MUD as well as performance improvement via exchanging correlation information during joint decoding process.

2.4 Coding and Modulation Schemes

In this section, some techniques and earlier works involved in this research are introduced, including BICM-ID principle, doped accumulator, QPSK demapper and irregular repetition code.

2.4.1 BICM-ID Principle

The basic BICM principle is first proposed by Zehavi in [6], with a purpose of increasing the diversity order of the trellis-coded-modulation modulation [7]. It performs a bit-level interleaver rather than symbol-level at the transmitter side.

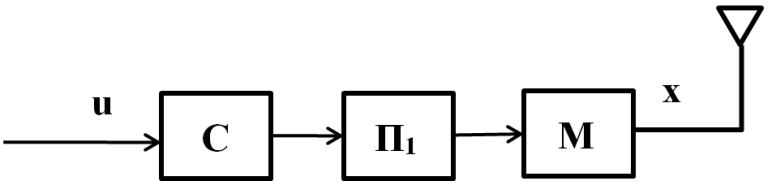

(a) BICM-ID transmitter model

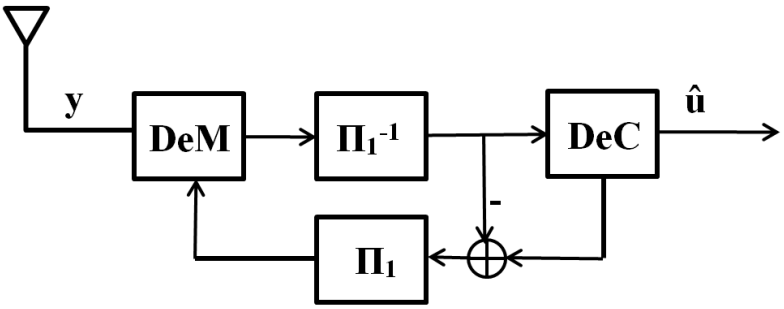

(b) BICM-ID receiver model

Figure 2.5. BIDM-ID Transmitter and Receiver Model

At the receiver side, in order to improve decoding performance, Li and Ritcey apply the iterative decoding process, which is provided in [8] and is called BICM-ID. Based on the turbo principle, *extrinsic* LLRs are exchanged between decoder and demapper to obtain more information about u. The basic system model of BICM-ID is illustrated in Fig. 2.5. If we remove the feedback in Fig. 2.5(b), it becomes the original BICM receiver model.

It should be noticed that non-Gray mapping, rather than Gray mapping, is more suitable to BICM-ID scheme. To verify the suitability, the QPSK with Gray and non-Gray mapping is used as an example, as shown in Fig. 2.6. By comparing these two cases, the Euclidean distance between two constellation points of the

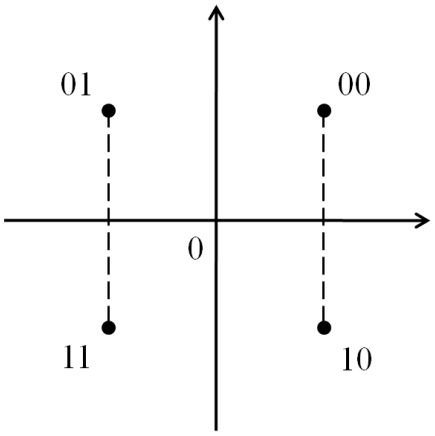

(a) Constellation distance of first bit in QPSK with Gray mapping

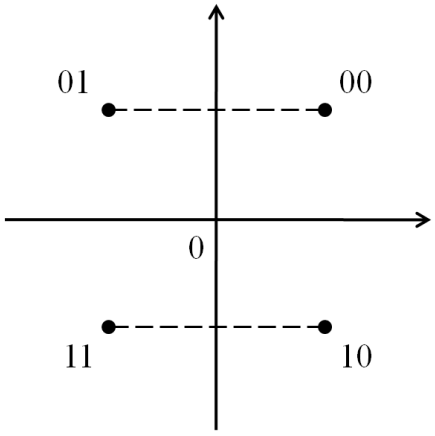

(b) Constellation distance of second bit in QPSK with Gray mapping

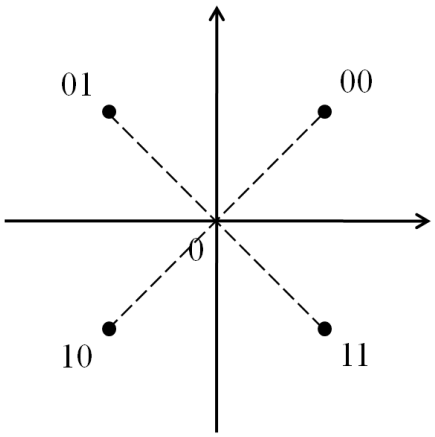

(c) Constellation distance of first bit in QPSK with non-Gray mapping

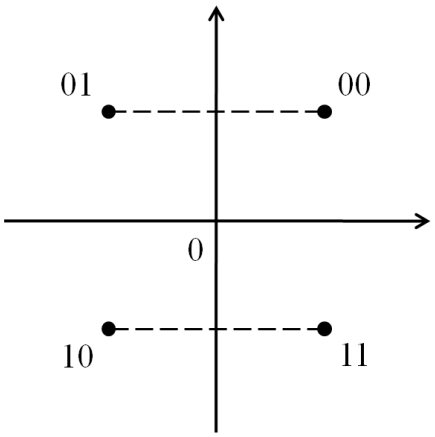

(d) Constellation distance of second bit in QPSK with non-Gray mapping

Figure 2.6. QPSK Constellations with Gray and Non-Gray Mmapping

second bit shown in Fig. 2.6(b) and 2.6(d) are the same in Gray and non-Gray cases. However, the Euclidean distance of the first bit with non-Gray mapping is larger than that with Gray mapping. Similar result also can be found for 8PSK as well [7].

Additionally, from system structure point of view, we can find that the structure of BICM-ID is naturally suitable to the IDMA. Comparing Fig. 2.5(a) and the left side of Fig. 2.1, it is obvious that the BICM-ID has similar structure as the IDMA at transmitter side. Therefore, BICM-ID principle can be easily applied into IDMA system so that benefits of IDMA and BICM-ID, which is introduced in section 2.1 and this section, can be exploited in the system.

2.4.2 Doped Accumulator

The doped accumulator [27] has the same structure as the memory-1 RSC code encoder, as shown in Fig. 2.7.

The output of DACC with a specified doping ratio Q is a mixture of systematic bits and coded bits, where every Q-th bits in the systematic bit sequence are replaced by the corresponding coded bits in the coded sequence. It should be noticed that the overall code of DACC is 1 and thus DACC has no error correcting capability at all. However, the DACC can help to reshape the EXIT chart curve of demapper to improve the convergence property, as shown in Fig. 2.8 [28] and will be discussed in Section 2.2.4.

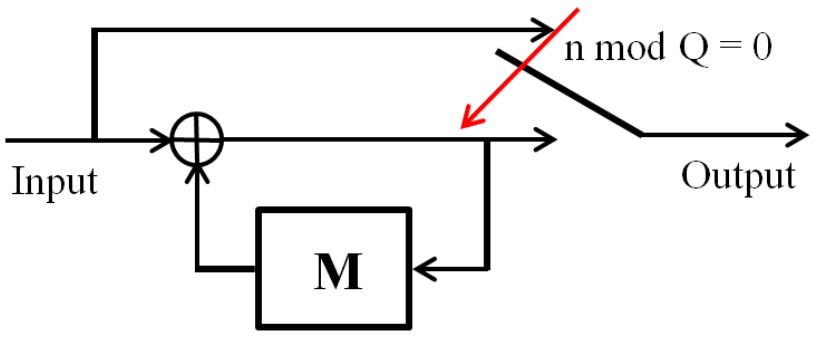

Figure 2.7. Structure of Doped Accumulator with Doping Ratio Q

2.4.3 QPSK Demapper

In this research, QPSK is used as the modulation scheme. As we have discussed in Section 2.4.1, non-Gray mapping is performed as the mapping scheme. Therefore, a demapper is required to compute LLR for coded bits. The MAP algorithm is performed to compute the *extrinsic* information. The *extrinsic* LLR $L_{e,Dem}$ of d-th bit in m-th symbol can be computed by

$$L_{e,Dem}[b_d] = \ln \frac{\sum_{x_m \in S_1} e^{-\frac{|y_m - x_m|^2}{\sigma^2}} \prod_{q=1, q\neq d}^{2} e^{b_q L_{a,Dem,b_q}}}{\sum_{x_m \in S_0} e^{-\frac{|y_m - x_m|^2}{\sigma^2}} \prod_{q=1, q\neq d}^{2} e^{b_q L_{a,Dem,b_q}}}, \tag{2.18}$$

where b_d is d-th bit in m-th symbol, $S_1(S_0)$ and b_q are labelling set and corresponding q-th bit ($q \neq d$) with d-th bit being 1(0), L_{a,Dem,b_q} is *a priori* information fed back form the decoder, σ^2 is the Gaussian noise variance, y_m is the received symbol and x_m is the constellation point of $S_1(S_0)$, respectively.

2.4.4 EXIT Chart Analysis

EXIT chart is a technique that help construct good iteratively-decoded error-correcting codes and is developed by Stephan ten Brink on the concept of *extrinsic* information exchange [29]. It is an very useful tool to analyse the convergence property of iterative decoding process and help the optimization of coding and modulation schemes.

EXIT chart uses mutual information to show how iterative decoding is performed via exchanging *extrinsic* information between decoding components. If there are two components exchanging *extrinsic* information, the convergence property of components can be plotted using a 2D EXIT chart. Similarly, 3D EXIT chart can be used to analyse convergence property when there are three components. In the 2D EXIT chart, input *a priori* mutual information of one component is plotted on the horizontal axis and the corresponding output *extrinsic* information is on the vertical axis, while the definition of the axis for another component is opposite. If there is a tunnel between two EXIT curves in 2D case, or 3 planes in 3D case, of the components in the EXIT chart, the *extrinsic* mutual information monotonically increases via iterations. No more *extrinsic* mutual informations is obtained when two curves intersect with each other. However, if the intersection happens at the (1, 1) point, it means the receiver can successfully decode the

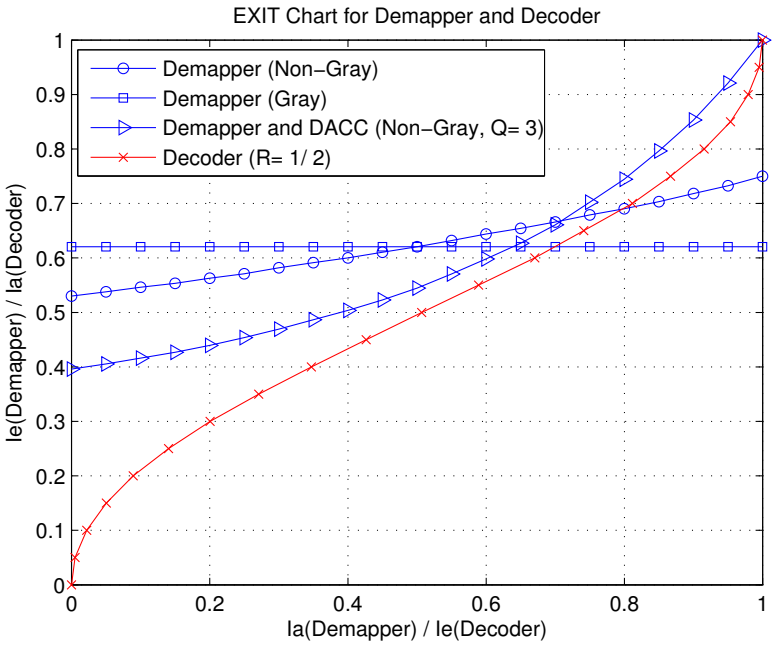

Figure 2.8. EXIT Chart of Demapper and Decoder at $SNR = 2dB$

original information.

In this subsection, we explain more details about comparison between Gray and non-Gray mapping, and the benefit of DACC by using EXIT chart analysis. Fig. 2.8 is an example of the EXIT chart of demapper and decoder at $SNR = 2dB$, where the horizontal axis is the demapper *a priori* mutual information $\mathbf{I}^c_{a,Dem}$ and the decoder *extrinsic* mutual information $\mathbf{I}^c_{e,Dec}$ while the vertical axis is the demapper *extrinsic* mutual information $\mathbf{I}^c_{e,Dem}$ and the decoder *a priori* mutual information $\mathbf{I}^c_{a,Dec}$, where L_a and L_e donate *a priori* LLR and *extrinsic* LLR of decoding compnents, respectively. From the observation of the two curves marked with circle and square in Fig. 2.8, it can be found that the $\mathbf{I}^c_{e,Dem}$ of the curve of non-Gray mapping will increase according to the increase of $\mathbf{I}^c_{a,Dem}$ by iteration. Therefore, BICM-ID with non-Gray mapping can achieve better system performance than Gray mapping. However, even though the non-Gray mapping outperforms the Gray mapping, intersection of the demapper curve and the decoder curve happens before the *extrinsic* mutual information of decoder reaching the (1, 1) point, as shown in Fig. 2.8. With the help of DACC, the tunnel between demapper curve and decoder curve keep open and the both can finally reach the (1, 1) point, meaning that decoder can successfully decode the original information, as shown in the

curve marked with triangle and circle in Fig. 2.8.

In the chapter 4, we will use EXIT chart to analyse the convergence property of correlated sources transmitted over MAC and joint decoding process.

2.4.5 Coding and Decoding scheme

The channel code used in this research is irregular repetition code which is a modified version of conventional repetition code. There is a set indicating repetition times in an IrR encoder. In this research, we will use the expression described in Equ. (2.19) to define the set for an IrR the encoder:

$$\mathbf{d} = [d_1, d_2, \cdots] \quad \text{and} \quad \mathbf{p} = [p_1, p_2, \cdots], \tag{2.19}$$

where d_k, $k \in \{1, 2, \cdots\}$, is repetition coefficients and p_k, $k \in \{1, 2, \cdots\}$, is the percentage of bits which will be repeated d_k times in a codeword.

For example, an IrR encoder is defined as

$$\mathbf{d} = [2, 3] \quad \text{and} \quad \mathbf{p} = [0.5, 0.5]. \tag{2.20}$$

In this example, 50% bits are repeated twice and another 50% bits are repeated three times to generate codewords. The overall code rate of this IrR code is 0.4. It is important that bits, which will be repeated d_k times, are chosen randomly from the information sequence.

The decoding function for IrR code is same as conventional repetition code, which can be expressed as

$$L^c_{p,Dec,m} = \sum_{d=1}^{D} L^c_{a,Dec,d} + L^u_{a,Dec,m}, \tag{2.21}$$

where $L^c_{p,Dec,m}$ is the *a posteriori* LLR for m-th coded bit whose repetition time is D in the encoder while $L^c_{a,Dec,d}$ and $L^u_{a,Dec,m}$, $d \in \{1, 2, \cdots D\}$, are the *a priori* LLR for the codeword, which contains m-th bit, and its corresponded information bit.

Regarding the DACC discussed in Section 2.4.2, since it has the same structure as the memory-1 RSC encoder, a decoder is required for decoding the input of DACC at the receiver side. In this research, *a posteriori* probability decoding is

assumed to recover the systematic information input to DACC, from which the *a posteriori* LLR can be computed by Equ. (2.22).

$$L_{p,DACC} = \ln \frac{P(x=1|y)}{P(x=0|y)}. \tag{2.22}$$

The algorithm used in the decoder is referred to the BCJR algorithm [30]. The BCJR algorithm is a standard operation for decoding trellis-based codes, therefore, we will not discuss the decoding process in details in this thesis.

2.5 Summary

In this chapter, several basic principles and problems to be investigated in this research, such as IDMA, correlated sources and BICM-ID, have been briefly introduced. The mathematical expression of AGWN channel, frequency selective fading channel and MAC were provided as well as their properties. Moreover, structure and purpose of some key techniques and algorithms used in this research such as DACC, demapper and coding-decoding algorithms, were introduced. The result of the investigations in this chapter will be used to construct the system in this thesis.

Chapter 3

Impact Investigation of Source Correlation

3.1 Introduction

In cooperative communications, source correlation is a non-negligible part and sometimes can be utilized in the decoding process. In the future communications, instead of using orthogonal MAC, it is quite likely that for this purpose, non-orthogonal MAC has to be taking into account in order to increase the transmission efficiency. However, the impact of source correlation on MUD under non-orthogonal MAC should be first investigated. In this chapter, the correlation impact on system performance is investigated by setting source correlation as a parameter. Since the SSIC is the most promising technique, the impact of source correlation on SSIC is investigated in this chapter, where the decoding process is performed independently user-by-user. Hence, in this chapter, our investigation is only on the SSIC performance.

First of all, basic system model and its component functions are provided to introduce as a knowledge basis of investigation. Then, the structure of the FD-SC-MMSE channel equalizer is introduced, and the modified system model under frequency selective fading channel is provided. After that, numerical results are provided under AWGN channel and frequency selective fading channel assumptions. Finally, discussion and conclusion of this chapter are given.

3.2 System Model

In this section, the system model for investigating impact of source correlation on IDMA-based MUD under the AWGN channel assumption is proposed. First of all, the correlated source generation and transmission scheme are introduced. After that, the expression of received signal is given. Then, the MUD and decoding schemes are provided, including iteration scheme, SSIC, modified demapper function and decoding scheme.

The basic IDMA-based MUD system model is depicted in Fig. 3.1. With this model, the MAC channel suffers from only AWGN component. System model under frequency selective fading channel assumption will be discussed in Section 3.3.

3.2.1 Transmission Scheme

At the transmitter side, we first generate the correlated sources. For the case of analysis, the number K of correlated sources is always set to 2 in this thesis. In this case, the bit-flipping model is used for generating correlated sources. The parameter p_e in Fig. 3.1(a) is referred to percentage of flipped bits, or called intra-link error probability in some materials, in the original information sequence u. The process of bit-flipping can be expressed as

$$u' = u \oplus e, \tag{3.1}$$

where u is original binary information sequence with length N_u, e is a binary error vector with length N_u and has $N_u \cdot p_e$ 1s which are randomly allocated. Information sequence for user-1 u_1 is same as u, while u_2 is generated by passing the bit-flipping function and an interleaver Π_0. The information sequence u_k for k-th user, where $k \in \{1, 2\}$, is first sent to an IrR encoder, followed by the user-specified interleaver Π_k, DACC and non-Gray QPSK mapper to generate the modulated symbol sequence x_k. After that, the modulated symbol sequence x_k is transmitted over MAC to the receiver.

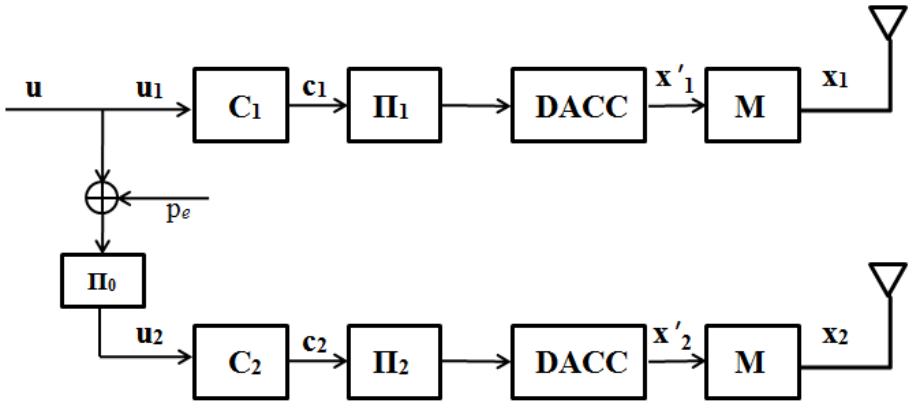

(a) BICM-ID transmitter model

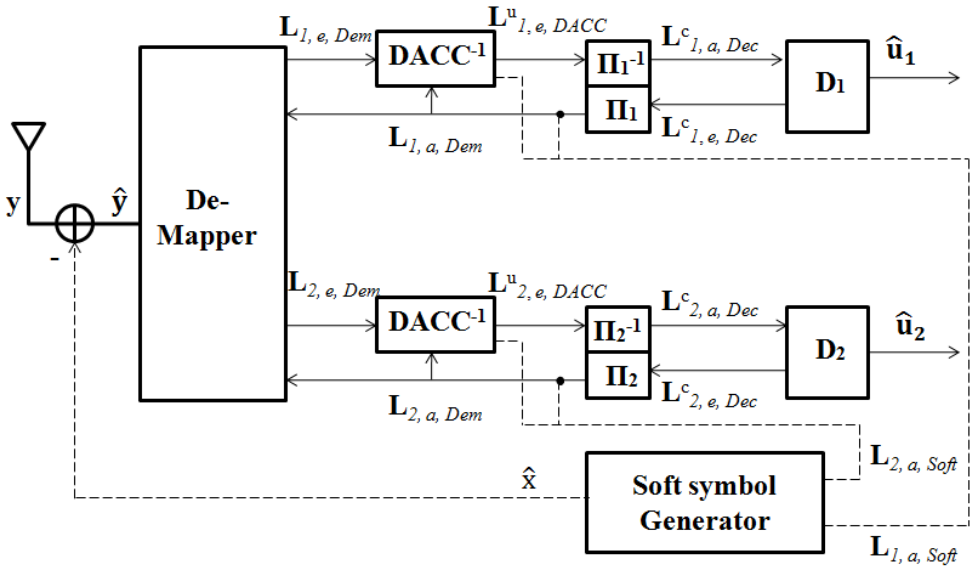

(b) BICM-ID receiver model

Figure 3.1. IDMA-based MUD System Transmitter and Receiver Model

3.2.2 MUD and Decoding Schemes

At the receiver side, the received signal $\mathbf{y}$ can be expressed as

$$\mathbf{y} = \sum_{k=1}^{K} \sqrt{P_k} \cdot \mathbf{x_k} + \mathbf{n}, \tag{3.2}$$

where P_k and $\mathbf{n}$ are the transmission power of the k-th user and AWGN component with variance σ_n^2, respectively. As we mentioned in Section 2.1, received signal also can be expressed as

$$\mathbf{y} = \sqrt{P_k} \cdot \mathbf{x}_k + \zeta_k \tag{3.3}$$

with

$$\zeta_k = \sum_{g=1, g\neq m}^{K} \sqrt{P_g} \cdot \mathbf{x}_g + \mathbf{n}. \tag{3.4}$$

Then the iterative multi-user detection and decoding process are performed to eliminate MAI and decode the original information for the 1st user and the 2nd user.

At the receiver, as shown in Fig. 3.1(b), the iteration in the MUD and decoding process are divided into two types. The solid line is referred to decoding process for decoding information, while the dashed line is referred to SSIC process for eliminating MAI, which are called local iteration and global iteration in this research, respectively. The iteration scheme, in general, in this research is that the global iteration will be activated once after several rounds of local iteration.

Local Iteration

The local iteration is performed among demapper, DACC decoder and IrR decoder. In the local iteration, the *a priori* LLR of coded bits to demapper and DACC decoder is initialized as 0 in the first iteration. And in this chapter, the *a priori* LLR of information bits to IrR decoder is always set as 0. The decoding functions for DACC and IrR code performed in the local iteration is provided by Equ. (2.22) and Equ. (2.21). It should be noticed that informations exchanged among local iteration components, as well as in the global iteration, are *extrinsic* information only, which can be computed by

$$\mathbf{L}_e = \mathbf{L}_p - \mathbf{L}_a, \tag{3.5}$$

where $\mathbf{L}_e$, $\mathbf{L}_p$ and $\mathbf{L}_a$ donate the *extrinsic* LLR, *a posteriori* LLR and *a priori* LLR, respectively.

Global Iteration

After several rounds of local iteration, the global iteration is activated, which is referred to the dashed lines, soft symbol generator and SSIC. The purpose of global iteration is to eliminate the MAI in the composite received signal by SSIC process. Because of that, the local iteration for each user can get more reliable *extrinsic* information from the demapper.

The first step of global iteration is to generate the soft replica of transmitted symbol sequence $\mathbf{x}$. For k-th user, whose transmission power is P_k, the $\mathbf{L}_{k,a,Soft}$ is the *a priori* LLR to soft symbol generator. The $\mathbf{L}_{k,a,Soft}$ is reconstructed from the *extrinsic* LLR of DACC decoder and IrR decoder in the last local iteration and should have exactly the same index arrangement as x'_k which is the input of the QPSK non-Gray mapper in Fig. 3.1(a). Then $\mathbf{L}_{k,a,Soft}$ are sent to the soft symbol generator to compute the soft symbol $\hat{\mathbf{x}}_k$ and the corresponded variance using Equ. (3.6) and Equ. (3.7).

$$\hat{x}_{k,m} = \sum_{s \in S} s \cdot \prod_{q=1}^{2} P(b_{k,q} = W) \tag{3.6}$$

$$\sigma^2_{k,m} = P_k - \hat{x}^2_{k,m} \tag{3.7}$$

with

$$P(b_{k,q} = W) = \frac{e^{b_{k,q} L_{k,a,Soft}}}{1 + e^{L_{k,a,Soft}}}, \tag{3.8}$$

where $W \in \{0, 1\}$, S is the set of constellation points. Before the first global iteration is activated, the soft symbol and its variance should be initialized as

$$\hat{x}_{k,m} = 0 \tag{3.9}$$

$$\sigma^2_{k,m} = 1. \tag{3.10}$$

Then the SSIC is performed to eliminate the interference. The process of SSIC is to subtract soft symbols of interference components from composite received signal and can be expressed as

$$\hat{y}_{k,m} = y_m - \hat{\zeta}_{k,m}, \tag{3.11}$$

where

$$\hat{\zeta}_{k,m} = \sum_{g=1}^{K} \sqrt{P_g} \cdot \hat{x}_{g,m} - \sqrt{P_k} \cdot \hat{x}_{k,m}. \tag{3.12}$$

The variance of interference experienced by k-th user after soft cancellation can be computed using

$$\sigma^2_{k,\zeta,m} = \sum_{g=1,g\neq k}^{K} P_g \cdot \sigma^2_{k,m} + \sigma^2_n. \tag{3.13}$$

After the SSIC, $\hat{\mathbf{y}}_k$ and its corresponding variance $\sigma^2_{k,\zeta}$ are sent to demapper to compute $\mathbf{L}_{k,e,Dem}$. Since the input signal and variance of demapper are not obtained directly from the channel in this system, the demapper function, originally provided by Equ. (2.18), is modified so that it matches the model, as

$$L_{k,e,Dem}[b_d] = \ln \frac{\sum_{x_{k,m}\in S_1} e^{-\frac{|\hat{y}_{k,m}-x_{k,m}|^2}{\sigma^2_{k,\zeta,m}}} \prod_{q=1,q\neq d}^{2} e^{b_q L_{a,Dem,b_q}}}{\sum_{x_{k,m}\in S_0} e^{-\frac{|\hat{y}_{k,m}-x_{k,m}|^2}{\sigma^2_{k,\zeta,m}}} \prod_{q=1,q\neq d}^{2} e^{b_q L_{a,Dem,b_q}}}, \tag{3.14}$$

where $\hat{\mathbf{y}}_k$ and $\sigma^2_{k,\zeta}$ are updated in every global iterations. The computational complexcity of demapper function can be reduced in log-domain by using Jacobi logarithm [31].

Then the *extrinsic* LLR of demapper is sent to DACC decoder with the *a priori* LLR fed back from channel decoder to start the next round of local iteration. It should be noticed that the *a priori* LLR of demapper and DACC decoder is the same and is reconstructed from the *extrinsic* LLR of IrR decoder.

3.3 Joint Turbo Equalizaion and MUD scheme

In the previous section, we have introduced the system model under AWGN channel assumption. In this section, channel assumption is extended to frequency selective fading channel, where both MAI and ISI exist. Therefore, a channel equalizer is required to eliminate ISI. We will first introduce the circulant channel matrix. And then, the structure and details of the *joint FD-SC-MMSE equalizer and demapper* are provided.

3.3.1 Channel Matrix

Cyclic prefix (CP) is assumed here as the prefix in transmission frame. Since the CP is appended at the transmitter side and removed at the receiver side, the channel matrix $\mathbf{H}$ is equivalent to a circulant matrix $\mathbf{H}^c$. The circulant channel matrix of the k-th user can be expressed as

$$\mathbf{H}_k^c = \begin{pmatrix} h_{k,0} & 0 & \cdots & h_{k,L-1} & \cdots & h_{k,2} & h_{k,1} \\ h_{k,2} & h_{k,0} & \cdots & 0 & \cdots & h_{k,3} & h_{k,2} \\ \vdots & \vdots & \ddots & \vdots & \ddots & \vdots & \vdots \\ h_{k,L-1} & h_{k,L-2} & \cdots & 0 & \cdots & 0 & h_{k,L-1} \\ 0 & h_{k,L-1} & \cdots & 0 & \cdots & 0 & 0 \\ \vdots & \vdots & \ddots & \vdots & \ddots & \vdots & \vdots \\ 0 & 0 & \cdots & h_{k,L-3} & \cdots & h_{k,0} & 0 \\ 0 & 0 & \cdots & h_{k,L-2} & \cdots & h_{k,1} & h_{k,0} \end{pmatrix}, \tag{3.15}$$

where $\mathbf{H}_k^c \in \mathbb{C}^{N_s \times N_s}$ and $h_{k,l}$ is the channel gain of l-th path of channel for the k-th user with N_s being the block length and L being the channel length. Then, the received signal described in Equ. (3.2) can be rewritten as

$$\mathbf{y} = \sum_{k=1}^{K} \quad \mathbf{H}_k^c \cdot \sqrt{P_k} \cdot \mathbf{x_k} + \mathbf{n}. \tag{3.16}$$

One important property of circulant matrix is that the $\mathbf{H}_k^c$ can be diagonalized by the DFT matrix, as shown in Equ. (3.17).

$$\mathbf{H}_k^c = \mathbf{F}^H \, \mathbf{\Xi}_k \, \mathbf{F}, \tag{3.17}$$

where $\mathbf{F} \in \mathbb{C}^{N_s \times N_s}$ is the normalized DFT matrix and $\mathbf{F}^H$ is the Hermitian transpose of $\mathbf{F}$. The diagonal components of matrix $\mathbf{\Xi}_k$ is the N_s-point DFT of the channel impulse response of k-th user which can be computed by the fast Fourier transform efficiently, as expressed in Equ. (3.18).

$$diag\{\mathbf{\Xi}_k\} = \mathcal{FFT}\{[\mathbf{h}_k, \mathbf{0}_{N_s-L}]\}. \tag{3.18}$$

Hence, $\mathbf{\Xi}_k$ also can be considered as the frequency domain expression of channel matrix.

3.3.2 Joint FD-SC-MMSE Equalizer and Demapper

To eliminate the ISI caused by multipath propagation, channel equalization is required at the receiver. There are various techniques for channel equalization, such as zero-forcing, MMSE and MLSE [16]. Due to the noise enhencement problem of zero-forcing and heavy computional complexity of MLSE, in this research, FD-SC-MMSE equalizer is considered as the channel equalization technique, which can avoid the noise enhencement without heavy computational complexity. The algorithm of this FD-SC-MMSE equalizer is provided in [32].

In frequency selective fading channels, the demapper at the receiver in Fig. 3.1(b) is replaced by a *joint FD-SC-MMSE equalizer and demapper*, which is illustrated in Fig. 3.2. Since the channel easimation is not the aim of this research, the channel estimator in the block diagram is assumed to provided the perfect output, indicating that the estimated $\hat{\mathbf{H}}_k$ is exactly equal to the true $\mathbf{H}_k$. The input $\hat{\mathbf{x}}_k$ is provided from the soft symbol generator. And the $\hat{\mathbf{y}}_k$ and σ_k^2 are the symbol sequence and the corresponding variance after SSIC. The process of SSIC under frequency selective fading channel assumption is obtained from Equ. (3.11) and Equ. (3.13) in AWGN channel, where the channel matrix should be considered here and equations are given as

$$\hat{\mathbf{y}}_k = \mathbf{y} - \sum_{g=1, g\neq k}^{K} \mathbf{H}_k^c \cdot \sqrt{P_g} \cdot \hat{\mathbf{x}}_g \tag{3.19}$$

$$\sigma_{k,\zeta}^2 = \sum_{g=1, g\neq k}^{K} E_g \cdot P_g \cdot \sigma_k^2 + \sigma_n^2, \tag{3.20}$$

where $\mathbf{H}_k^c$ is the circulant channel matrix and E_g is the channel total energy for the k-th user defined as

$$E_g = \sum_{l=0}^{L-1} |h_{g,l}|^2. \tag{3.21}$$

The input to the MMSE filter $\tilde{\mathbf{y}}$ is soft cancellation input, given by

$$\tilde{\mathbf{y}} = \hat{\mathbf{y}}_k - \mathbf{H}_k^c \cdot \sqrt{P_k} \cdot \hat{\mathbf{x}}_k. \tag{3.22}$$

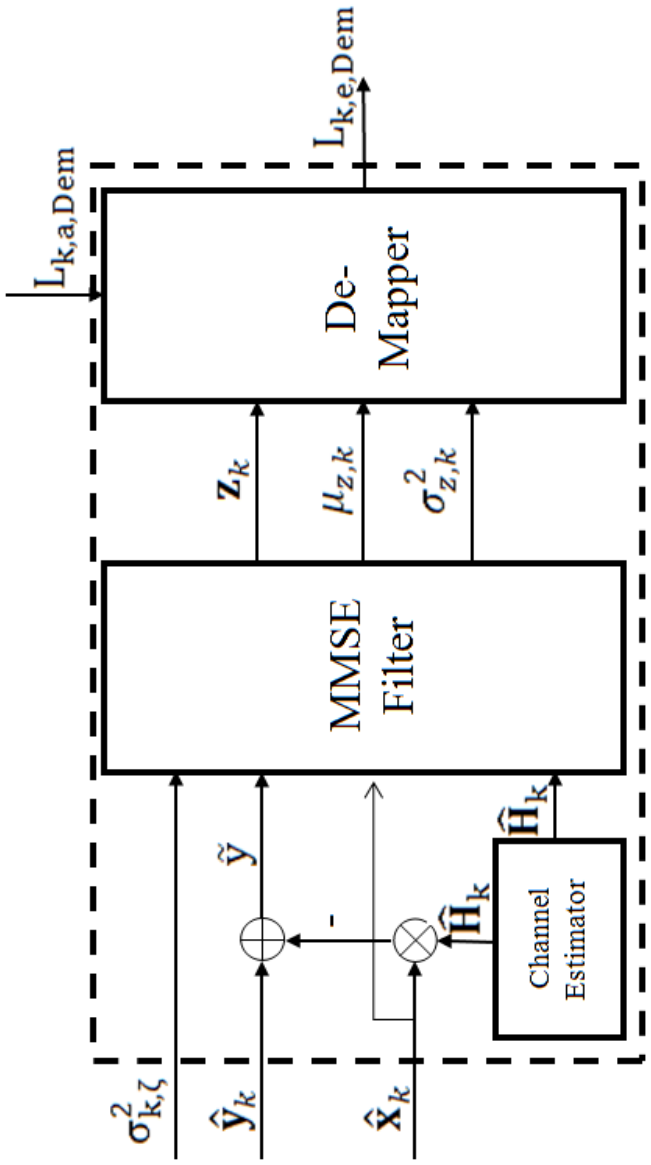

Figure 3.2. Structure of Joint FD-SC-MMSE Equalizer and Demapper

MMSE filter

After SSIC, $\hat{\mathbf{H}}_k^c$, $\hat{\mathbf{x}}_k$, $\tilde{\mathbf{y}}_k$ and $\sigma_{k,\zeta}^2$ are then forwarded to the MMSE filter. The output of MMSE filter can be expressed as

$$\mathbf{z}_k = (1 + \bar{\gamma}_k \bar{\delta}_k)^{-1} [\bar{\delta}_k \hat{\mathbf{x}}_k + \mathbf{F}^H \mathbf{\Psi}_k \tilde{\mathbf{y}}^f] \tag{3.23}$$

with the definition of $\bar{\gamma}_k$, $\bar{\delta}_k$, $\mathbf{\Psi}_k$ and $\tilde{\mathbf{y}}^f$ as follows:

$$\begin{aligned}
\bar{\gamma}_k &= \frac{1}{N_s} \mathrm{tr} \left[\Xi^H (\Xi \mathbf{\Delta} \Xi^H + \sigma_{k,\zeta}^2 \mathbf{I}_{N_s})^{-1} \Xi \right] && (3.24) \\
\bar{\delta}_k &= \frac{1}{N_s} \sum_{m=1}^{N_s} |\hat{x}_{k,m}|^2 && (3.25) \\
\mathbf{\Psi}_k &= \Xi^H (\Xi \mathbf{\Delta} \Xi^H + \sigma_{k,\zeta}^2 \mathbf{I}_{N_s})^{-1} && (3.26) \\
\tilde{\mathbf{y}}^f &= \mathbf{F} \cdot \tilde{\mathbf{y}}. && (3.27)
\end{aligned}$$

The $\mathbf{\Delta}$ is defined and approximated as follows:

$$\mathbf{\Delta} = \mathbf{F}\, \mathbf{\Lambda}\, \mathbf{F}^H \approx \frac{1}{N_s} \mathrm{tr} \mathbf{\Lambda} \cdot \mathbf{I}_{N_s} \tag{3.28}$$

with $\mathbf{\Lambda}$ being the symbol error covariance matrix as

$$\mathbf{\Lambda} = diag\{P_k - |\hat{\mathbf{x}}_k|^2\}. \tag{3.29}$$

Furthermore, the first and second moments of the MMSE filter output can be expressed as

$$\begin{aligned}
\mu_{z,k} &= \bar{\gamma}_k (1 + \bar{\gamma}_k \bar{\delta}_k)^{-1} && (3.30) \\
\sigma_{z,k}^2 &= \mu_{z,k} (1 - \mu_{z,k}). && (3.31)
\end{aligned}$$

Since we assume that the number of the receive antenna is one, except the DFT matrix $\mathbf{F}$, all of the N_s-by-N_s matrices in Equ. (3.23)-(3.29) are diagonal matrices. Hence, the computational complexity can be further reduced by only taking the diagonal components in practical equalization process.

Demapper

After the channel equalization, the equalizer output symbol sequence $\mathbf{z}_k$ is sent to the QPSK demapper. In this case, the demapper function provided in Equ. (3.14) should be further replaced by

$$L_{k,e,Dem}[b_d] = ln \frac{\sum_{x_{k,m} \in S_1} e^{-\frac{|z_{k,m} - \mu_{z,k} \cdot x_{k,m}|^2}{\sigma_{z,k}^2}} \prod_{q=1, q \neq d}^{2} e^{b_q L_{a,Dem,b_q}}}{\sum_{x_{k,m} \in S_0} e^{-\frac{|z_{k,m} - \mu_{z,k} \cdot x_{k,m}|^2}{\sigma_{z,k}^2}} \prod_{q=1, q \neq d}^{2} e^{b_q L_{a,Dem,b_q}}}. \tag{3.32}$$

It should be noticed that input from the MMSE filter $\mathbf{z}_k$, $\mu_{z,k}$ and $\sigma_{z,k}^2$ are updated every global iteration while the *a priori* LLR L_{a,Dem,b_q} is still updated every local iteration.

3.3.3 MUD and Decoding Scheme

The iterative MUD and decoding process in frequency selective fading channel, which is referred to the global iteration and the local iteration, is similar to what we have discussed in Section 3.2.2 for AWGN channel. It should be noted that even though the channel equalizer is performed with the demapper jointly, it is only activated in the global iteration because the soft symbol is updated in the global iteration only.

3.4 Numerical Reaults

In this section, a series of computer simulations are performed to investigate the impact of source correlation on IDMA-based MUD over AWGN channel and frequency selective fading channel, respectively. However, in this chapter, the decoding process is assumed to be performed independently user-by-user at the receiver. Hence, the source correlation is not utilized in the decoding process. The purpose of this chapter is to investigate if the source correlation results in impact on BER or FER performance in IDMA-based MUD, in the SSIC process only. The results can be shown by comparing BER curves or FER curves in AWGN channel and frequency selective fading channel, respectively, with different source correlation.

In the simulation, we use ρ to represent source correlation, which is defined as

$$\rho = 1 - 2p_e, \tag{3.33}$$

where p_e donates the bit-flipping probability. A series of ρ are investigated if there exits performance difference when different source correlation is given at the transmitter. Synchronous transmission is assumed in this research.

It should be noticed that the interleaver Π_0 at the transmitter is not necessary in this chapter, because decoding is performed independently user-by-user. It is shown that, in the simulation, the BER and FER performances are affected even if Π_0 is removed from the system model. However, it is still added at the transmitter in order to keep the consistency of system model with the next chapter where joint decoding process are assumed.

3.4.1 BER Performance in AWGN Channel

In this subsection, investigation in AWGN channel is first performed to obtain the basic investigation before multipath propagation is considered. In the AWGN channel, the power allocation is important since it dominates the signal to interference-plus-noise ratio (SINR) at the receiver, especially in high SNR region. According to the power allocation analysis of two users IDMA system in [12], it is shown that the unequal power allocation outperforms the equal power allocation in the AWGN channel. Hence, the unequal power allocation scheme is performed in the investigation in this subsection. Due to the unequal power allocation, the receive SNRs for different users are different and vary with their transmission power.

The parameters and algorithms used in the simulation are summarised in Table 3.1. The simulation results of BER performance for the 1st user and the 2nd user are illustrated in Fig. 3.3 and Fig. 3.4, respectively.

From Fig. 3.3, it can be found that, with different source correlation ρ, the proposed IDMA system achieves almost the same BER performance for the 1st user. The same result can also be found from Fig. 3.4 for the 2nd user case as well. It indicates that source correlation does not make any impact on BER performance directly in the purposed IDMA-based MUD system if decoding process is performed independently for each user.

This result can be considered as the benefit of the interleavers Π_1 and Π_2 in

the IDMA transmitter model. As mentioned above, the existence of Π_0 does not influence the result. In the discussion in this section, we assume that Π_0 does not pre-mutate the input sequence at all. In the system model, the sources sequences u_1 and u_2 have the correlation ρ. The correlation is also kept in coded sequences c_1 and c_2 since the channel encoder is deterministic function and has the same parameters for the 1st user and the 2nd user. However, the interleavers Π_1 and Π_2 in the IDMA transmitter is randomly generated for each user index. Therefore, the interleaved version of c_1 and c_2, as well as the transmitted symbol sequences x_1 and x_2, are statistically independent with each other. As a result, the source correlation is temporarily removed from the symbol sequences and does not make influence in the SSIC process which is performed at the symbol level.

Item	**Setting**
Source correlation (ρ)	{0, 0.25, 0.5, 0.75, 1}
Number of users (K)	2
Information Length (N_u)	10000
Number of Frames	3000
Channel Encoder	$\mathbf{d} = [3, 5]$
Parameters	$\mathbf{p} = [0.5, 0.5]$
Code rate (R)	1/4
Interleaver Type	Random interleaver
Dopping Ratio (Q)	2
Modulation Scheme	Non-Gray QPSK
Power Allocation	$P_1/P_2 = 1.5$
Demapping Algorithm	MAP algorithm
DACC and IrR Decoding Algorithm	MAP algorithm

Table 3.1. Parameters and algorithms for simulation in AWGN channel

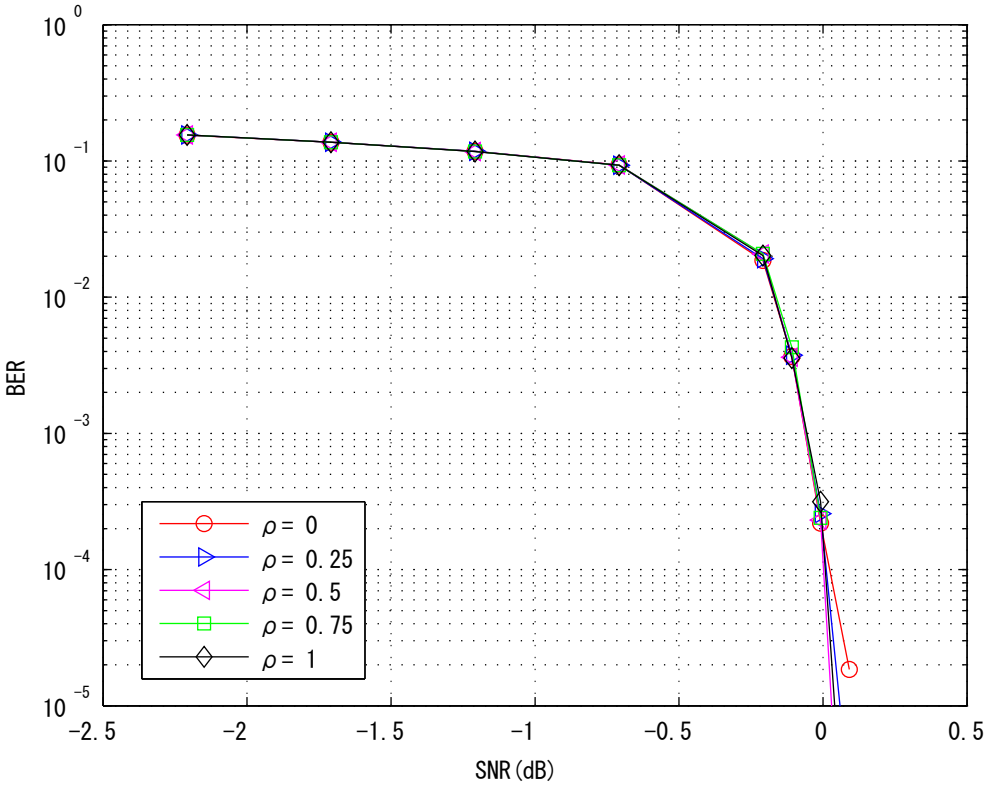

Figure 3.3. BER performance for the 1st user given different source correlation

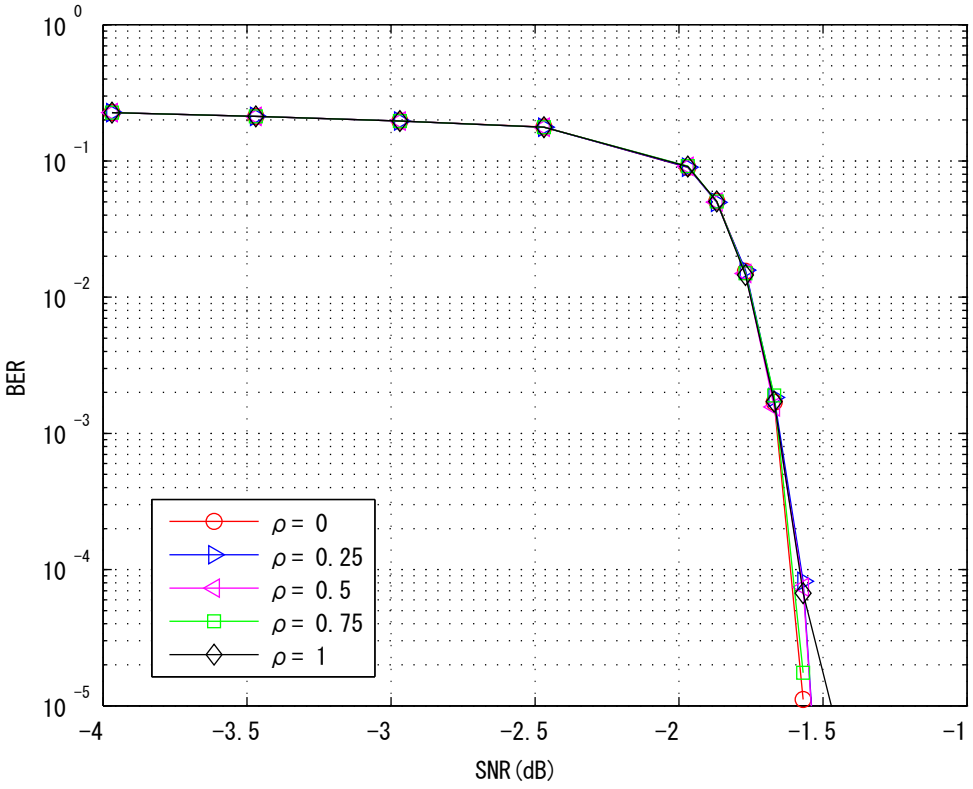

Figure 3.4. BER performance for the 2nd user given different source correlation

3.4.2 FER Performance in Frequency Seletive Fading Channel

After the investigation in AWGN, the channel assumption is extended to frequency selective fading channel in this subsection. In frequency selective fading channel, the channel gain is a random process. With 6-path channel assumed in this thesis, fading variation still remains and sometime cause deep fade, so that the transmission power is not the only fact to dominate the SINR at the receiver. For simplicity in investigation, the equal power allocation is assumed in this subsection.

Moreover, channel responses are generated randomly with expected value of channel energy equal to 1. Generally, long block length is needed to have the turbo equalizer works well. However, considering the assumption we have made in Chapter 2 that the channel impulse response stays the same within one transmission block, short transmission block length is required to hold the block fading assumption. Therefore, in the simulation, a relatively short block length is chosen in the simulation to take the balance to hold both two conditions. However, due to the randomness of the fading coefficients, in order to accurately evaluate the performance, more frames should be transmitted in the simulation in frequency selective fading channel.

The parameters and algorithms used in the simulation is summarised in Table 3.2. The FER curves for the 1st user and the 2nd user are illustrated in Fig. 3.5 and Fig. 3.6. It can be observed that nearly 6th order diversity can be achieved due to the channel length equal to 6.

From Fig. 3.5, it can be found that, regardless of the source correlation ρ, the IDMA system achieves almost the same FER performance for user-1. The same result can also be found from Fig. 3.6 for user-2 case as well. This result is the same as we have discussed in Section 3.4.1, which indicates that the explanation and conclusion we made in Section 3.4.1 is also valid under the frequency selective fading channel assumption.

Item	**Setting**
Source correlation (ρ)	{0, 0.25, 0.5, 0.75, 1}
Number of users (K)	2
Information Length (N_u)	1024
Number of Frames	100000
Channel Encoder	$\mathbf{d} = [3, 5]$
Parameters	$\mathbf{p} = [0.5, 0.5]$
Code rate (R)	1/4
Interleaver Type	Random interleaver
Dopping Ratio (Q)	2
Modulation Scheme	Non-Gray QPSK
Power Allocation	$P_1/P_2 = 1$
Channel length (L)	6
Equalization algorithm	MMSE estimation
Demapping Algorithm	MAP algorithm
DACC and IrR Decoding Algorithm	MAP algorithm

Table 3.2. Parameters and algorithms for simulation in frequency selective fading channel

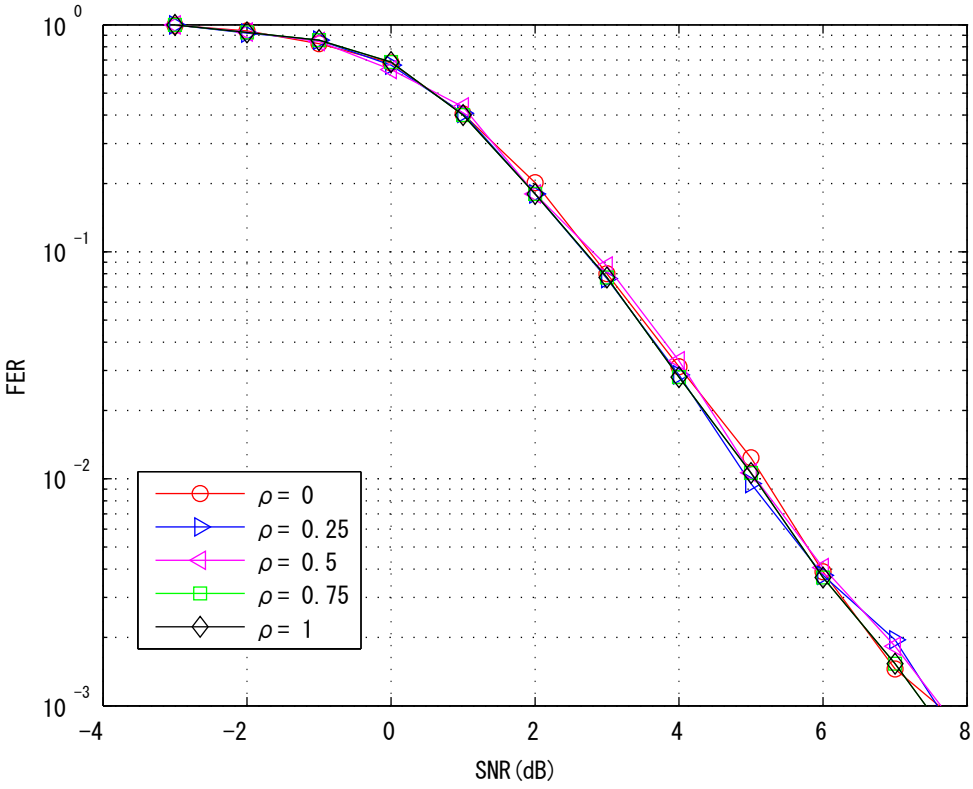

Figure 3.5. FER performance for the 1st user given different source correlation

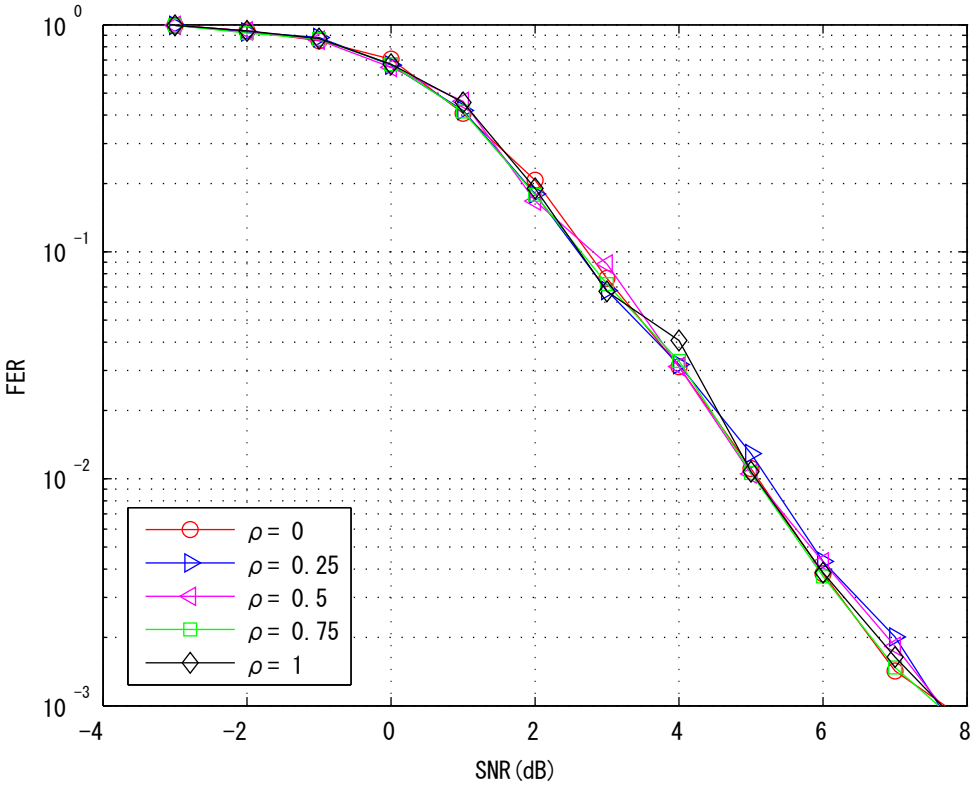

Figure 3.6. FER performance for the 2nd user given different source correlation

3.5 Summary

The primary objective of this chapter has been to investigate the impact of source correlation on IDMA-baed MUD with independent decoding at the receiver.

First of all, details of the system model, MUD structure and decoding scheme of the IDMA-based MUD system under AWGN channel assumption are introduced. After that, the structure of the *joint FD-SC-MMSE channel equalizer and demapper* is provided for eliminating ISI in frequency selective fading channel. Then the impact of source correlation over AWGN channel and frequency selective fading channel is investigated,where each user is independently decoded even though they are correlated. The corresponding BER and FER numerical performance results for AWGN channel and frequency selective fading channel, respectively, are provided.

From the BER and FER curves, it can be found that with help of interleavers in the IDMA transmitter the source correlation can be temporarily removed at the transmitted symbol level. Therefore, in the SSIC process, which is performed at the symbol level, informations from different users can be considered uncorrelated. The simulation results indicate that the source correlation does not make influence on BER and FER performance in the proposed IDMA-based MUD system if decoding process for each user is performed independently. In the next chapter, the joint decoding is performed to utilize the source correlation in decoding process in order to improve the BER and FER performance.

Chapter 4

Impact Investigation on Source Correlation with Joint Decoder

4.1 Introduction

In the previous chapter, we have investigated the impact of source correlation on IDMA-based MUD with independent decoding for each user. With the help of interleavers in the IDMA transmitter, the source correlation can be temporarily removed at the symbol-level where the SSIC is performed. As a result, source correlation doesn't make influence on BER and FER performance in SSIC process, if decoding process is performed independently user-by-user. Therefore, it is natural to further investigate if it is possible to utilize the source correlation in the decoding process to improve system performance. It can be expected that system performance can be further improved by the exploitation of the correlation information between users.

In this chapter, joint decoding is performed at the receiver in order to utilize the source correlation to improve the system performance, where local, global and vertical iteration are involved. First of all, the system model is provided. Since the transmitter and receiver models are almost the same as that we have provided in the previous chapter, we will focus on the joint decoder in this chapter. Then, the benefit of performing joint decoding is investigated by using EXIT chart. After that, the numerical results are provided under the AWGN channel and the frequency selective fading channel assumptions. Finally, an analysis and a discussion on rate-sum / performance gain trade-off are provided by using the S-W region

and the MAC region analysis.

4.2 System Model

In this section, the system model is provided. The system model of transmitter and receiver in IDMA system are first briefly introduced. Then the structure of joint decoder is introduced. Since joint decoder can also be considered as vertical iteration structure, to reduce the times of iteration, a modified iteration scheme is discussed in this section as well.

The modified system model with joint decoder is depicted in Fig. 4.1. As we have discussed in the previous chapter, the receiver model in Fig. 4.1(b) is for the AWGN channel, while for the frequency selective fading channel the *demapper* is replaced by the *joint FD-SC-MMSE equalizer and demapper* to eliminate ISI. In this chapter, joint decoding is performed via a systematic LLR computation function, referred to *fc* function, in addition to, Π_0 and Π_0^{-1} as shown in Fig. 4.1. Since the transmission and MUD scheme are the same as we have provided in the previous chapter, in this chapter, only joint decoding scheme and the modified iteration scheme are introduced.

4.2.1 Joint Decoding scheme

In this subsection, the principle and the structure of joint decoder are introduced. As we mentioned above, joint decoding is referred to *fc* function, Π_0 and Π_0^{-1} in the receiver. In the Chapter 3, we have mentioned that Π_0 is not necessary in the transmitter model with independent decoding, however, it is required in this chapter to perform the vertical iteration. It should be noticed that the joint decoding is an iterative process, therefore, based on the turbo principle, an interleaver Π_0 is required between iteration components, which are referred to channel decoders for the 1st and the 2nd user in this case.

The core part of the joint decoder is the *fc* function. The *fc* function calculates the *a priori* LLRs of systematic bits for channel decoders, which were ignored in the previous chapter. The *extrinsic* LLRs of the systematic bits from the last local iteration and the intra-link error p_e are provided as inputs to the fc function. The

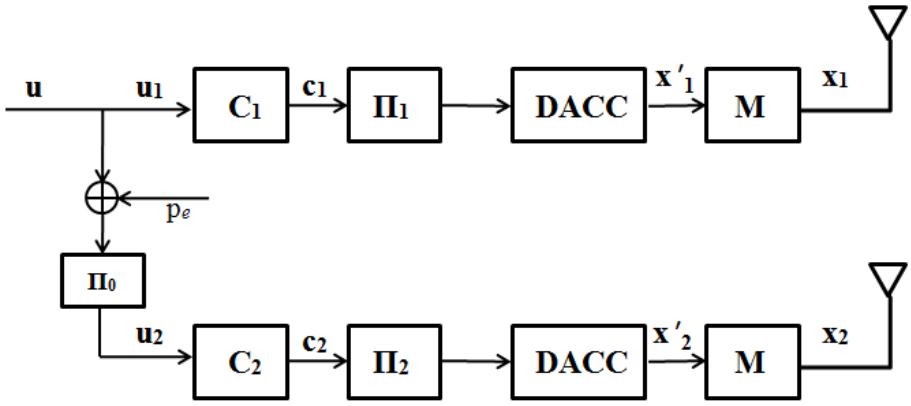

(a) BICM-ID transmitter model

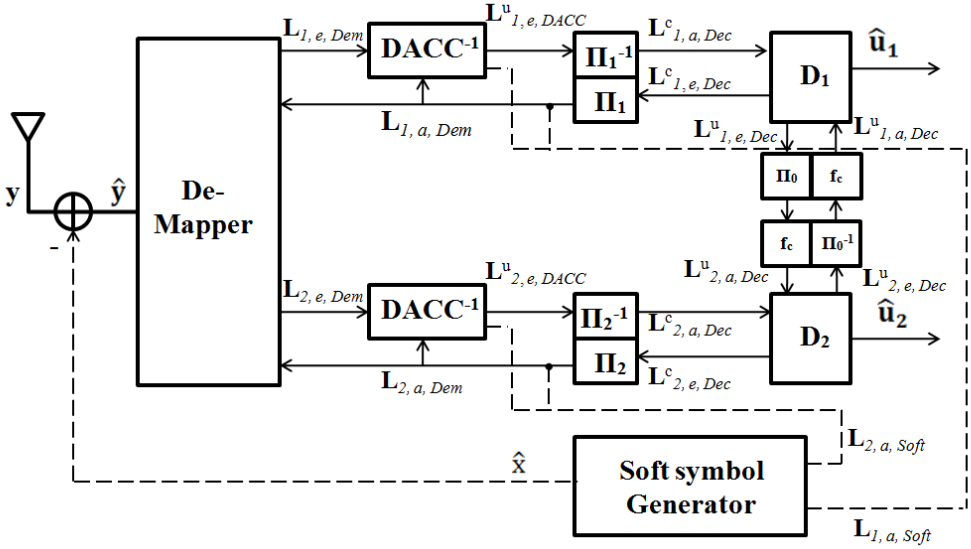

(b) BICM-ID receiver model

Figure 4.1. IDMA-based MUD System Transmitter and Receiver Model with Joint Decoder

output of the fc function is given as following:

$$f_c(x) = ln\ \frac{(1-p_e)\cdot\ e^x + p_e}{(1-p_e) + p_e\cdot\ e^x} \tag{4.1}$$

with x being

$$x = \Pi_0\ (L^u_{1,e,Dec}) \quad or \quad x = \Pi_0^{-1}\ (L^u_{2,e,Dec}), \tag{4.2}$$

where $\Pi_0\ (L^u_{1,e,Dec})$ and $\Pi_0^{-1}\ (L^u_{2,e,Dec})$ are the interleaved version of $L^u_{1,e,Dec}$ and the de-interleaved version of $L^u_{2,e,Dec}$, respectively, corresponding to the interleaver Π_0 used in the transmitter.

The source correlation, which is referred to the intra-link error probability p_e, is assumed to be known at the receiver in this theis. Therefore, the joint decoder can have the true p_e for decoding process. However, in the practical case, the receiver usually does not have the full knowledge about intra-link error p_e. In this case, p_e can be estimated by using the *a posteriori* LLRs, $\mathbf{L}^u_{1,p,Dec}$ and $\mathbf{L}^u_{2,p,Dec}$, of systematic bits from the channel decoders, as shown in Equ. (4.3) [33]. With the more iteration process, the more accurate estimated p_e can be obtained.

$$\hat{p}_e = \frac{1}{N}\sum_{n=1}^{N}\ \frac{e^{L^u_{1,p,Dec,n}} + e^{L^u_{2,p,Dec,n}}}{(e^{L^u_{1,p,Dec,n}}+1)(e^{L^u_{2,p,Dec,n}}+1)}. \tag{4.3}$$

The benefit of joint decoding is that it can provide the *a priori* LLR of systematic bits to the channel decoder to help the decoding process, which can be shown by using the EXIT chart. Since the channel decoder has two inputs and one output, the 3D EXIT chart is used in this section. Fig. 4.2 is the 3D EXIT chart of demapper and decoder with source correlation $\rho = 0.25$ and $\rho = 0.75$ when $SNR = 0dB$. In the Fig. 4.2, it can be found that, although the *a priori* mutual information of coded bits $\mathbf{I}^c_{a,Dec}$ is 0, with the help of the *a priori* mutual information of systematic bits $\mathbf{I}^u_{a,Dec}$ provided by the fc function, the output *extrinsic* mutual information $\mathbf{I}^u_{e,Dec}$ is larger than 0. It indicates that, with the help of $\mathbf{I}^u_{a,Dec}$, the decoder can provide larger output $\mathbf{I}^u_{e,Dec}$. The tunnel between decoder plant and demapper plant is larger if the fc finction can provide the larger $\mathbf{I}^u_{a,Dec}$ via iteration. Moreover, with relatively high source correlation, $\rho = 0.75$, as shown in Fig. 4.2(b), it can be seen that the joint decoder can significantly increase the $\mathbf{I}^u_{e,Dec}$ of decoder. However, with low source correlation, $\rho = 0.25$, as shown in Fig. 4.2(a), the $\mathbf{I}^u_{e,Dec}$ does not increase much even the $\mathbf{I}^u_{a,Dec}$ is close to 1. In the

both cases, the convergence tunnel is open until a point close to the $(1, 1, 1)$ mutual information point. This means that decoder can successfully recover the original information. This conclusion drawn from 3D EXIT chart can also be verified in the BER performance by computer simulation provided in Section 4.3.

4.2.2 Iteration Scheme

As we have discussed in the Chapter 3, the local iteration and the global iteration are performed to decode original information and eliminate the MAI, respectively. In this chapter, the basic local and global iteration schemes are the same. However, joint decoding includes vertical iteration which aims to exploit the correlation knowledge. Even though we know that it is necessary to control the activation ordering for the three types of iteration to eliminate the excessive iterations. This thesis takes the activation ordering as described below.

As stated before, that the local iteration is to decode the original information and is performed on the bit-level, while the global iteration is to eliminate the ISI and MAI and is performed on the symbol-level. In this chapter, we will follow the role to manage the iteration scheme. In addition to the local and global iterations, the vertical iteration is performed in the joint decoders, of which roles is to provide the systematic *a priori* LLRs for channel decoders with the aim of helping decoders with each other and is performed on the bit-level. Therefore, based on the role described above, we consider the vertical iteration process as a part of the joint decoding and is performed with the local iteration at the same time.

As a result, the iteration type in this chapter is still two, which are still called local iteration and global iteration in this chapter. The local iteration is first performed which includes demapping, DACC decoding, IrR decoding. Vertical iteration is then performed via *fc* function, Π_0 and Π_0^{-1}. After several rounds of local iterations and vertical iterations, the global iteration is performed to eliminate the interference components via the SSIC process.

4.3 Numerical Results

In this section, a series of computer simulations are performed to investigate the system performance when the source correlation is utilized in the decoding process. Basic simulation parameters and algorithms are the same as we used in the Chapter

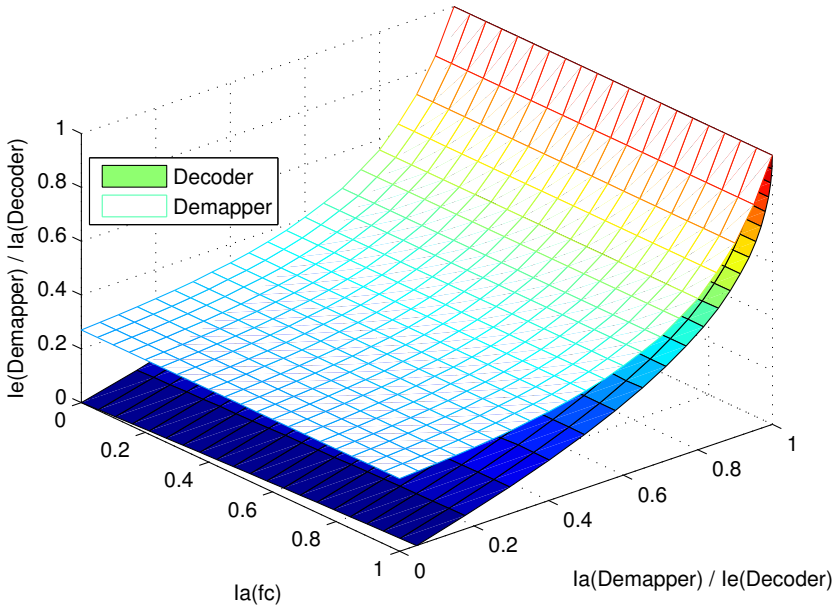

(a) EXIT chart for fc function with $SNR = 0dB$ and $\rho = 0.25$

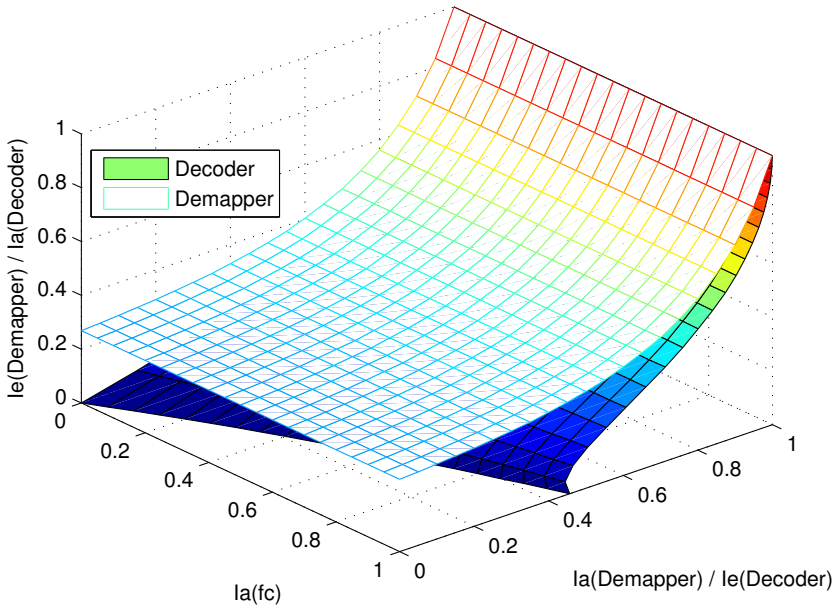

(b) EXIT chart for fc function with $SNR = 0dB$ and $\rho = 0.75$

Figure 4.2. 3D EXIT chart for demapper and IrR decoder with $SNR = 0dB$

3, as shown in Table 3.1 and Table 3.2. Simulations are performed under both AWGN channel and frequency selective fading channel assumption.

With source correlation $\rho = 0$, since sources are independent with each other, vertical iteration is not activated at the receiver in the simulation. The curves with $\rho = 0$ in the simulation results is plotted using dashed line as the baseline for system performance comparison.

The BER performance in AWGN channel is illustrated in Fig. 4.3 and Fig. 4.4 for the 1st user and the 2nd user, respectively. While, The FER performance in frequency selective fading channel is illustrated in Fig. 4.5 and Fig. 4.6 for the 1st user and the 2nd user, respectively.

4.3.1 AWGN channel

The BER performance in AWGN channel is illustrated in Fig. 4.3 and Fig. 4.4 for the 1st user and the 2nd user, respectively. From the simulation results, it is obvious that the BER performances become better with higher source correlation ρ.

In the Fig 4.3, it is found by comparing the curves with $\rho \neq 0$ with the dashed line corresponding to $\rho = 0$ of the 1st user, with low source correlation $\rho = 0.25$, the gap between the curve corresponding to $\rho = 0.25$ and the baseline, $\rho = 0$, is very small, only around $0.2dB$ gain. However, with relatively high source correlation $\rho = 0.75$, a significant gap , around $1.5dB$ gain can be achieved over the baseline. This indicates that the joint decoder can significantly improve the system performance. This result matches the conclusion we have drawn in Section 4.2.1 using the 3D EXIT chart. Moreover, with source correlation $\rho = 1$, in this case, the original information of two sources are the exactly same, hence, the SNR is twice as large as the case of $\rho = 0$. Hence a very large gain, around $3dB$, can be observed. Same conclusion can also be obtained for the 2nd user as well.

4.3.2 Frequency selective fading channel

The FER performance in frequency selective fading channel is illustrated in Fig. 4.5 and Fig. 4.6 for the 1st user and the 2nd user, respectively. From the simulation results, it is found that the larger correlation the better FER performances.

From the Fig. 4.5, similar conclusion can also be drawn as in Section 4.3.1. With low source correlation, the gap between solid curve and dashed curve is

very small, hence only a small performance gain can be achieved. While with large source correlation, a large gap can be observed, indicating that system performance improvement provided by the joint decoder is very significant. Moreover, since the channel length assumed in the simulation is 6, with the source correlation $\rho = \{0.25,\ 0.5,\ 0.75\}$, their corresponding curves can finally achieve nearly the 6th order diversity. However, with the source correlation $\rho = 1$, since two 6-path channels are transmitting the exactly same information, the curve can achieve nearly 6×2, which is the 12th order diversity. From the Fig. 4.5, a significant difference on the diversity order between the black curve, whose corresponding $\rho = 1$, and other curves can be observed. Same conclusion can also be drawn for the 2nd user as well.

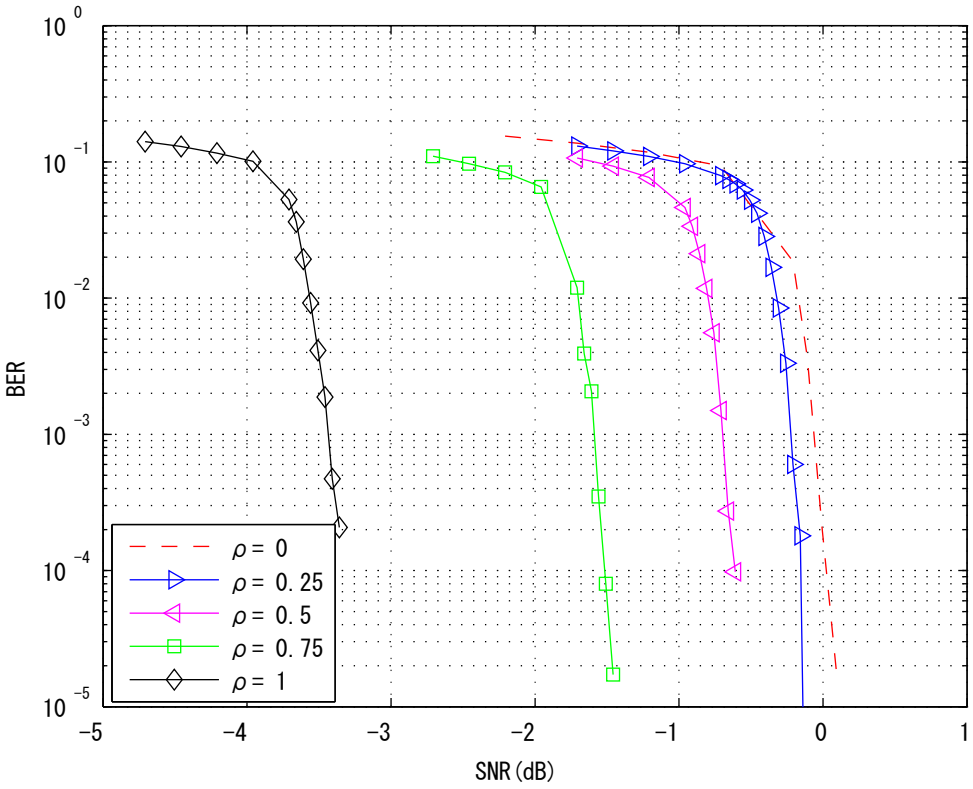

Figure 4.3. BER performance for the 1st user using joint decoder at the receiver

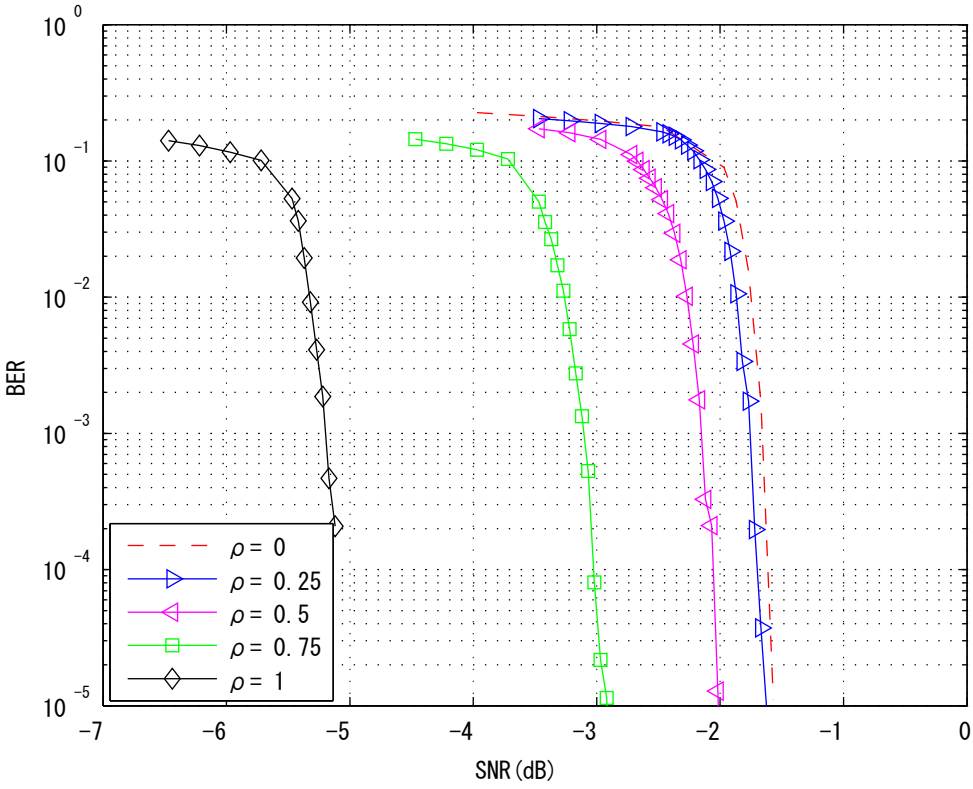

Figure 4.4. BER performance for the 2nd user using joint decoder at the receiver

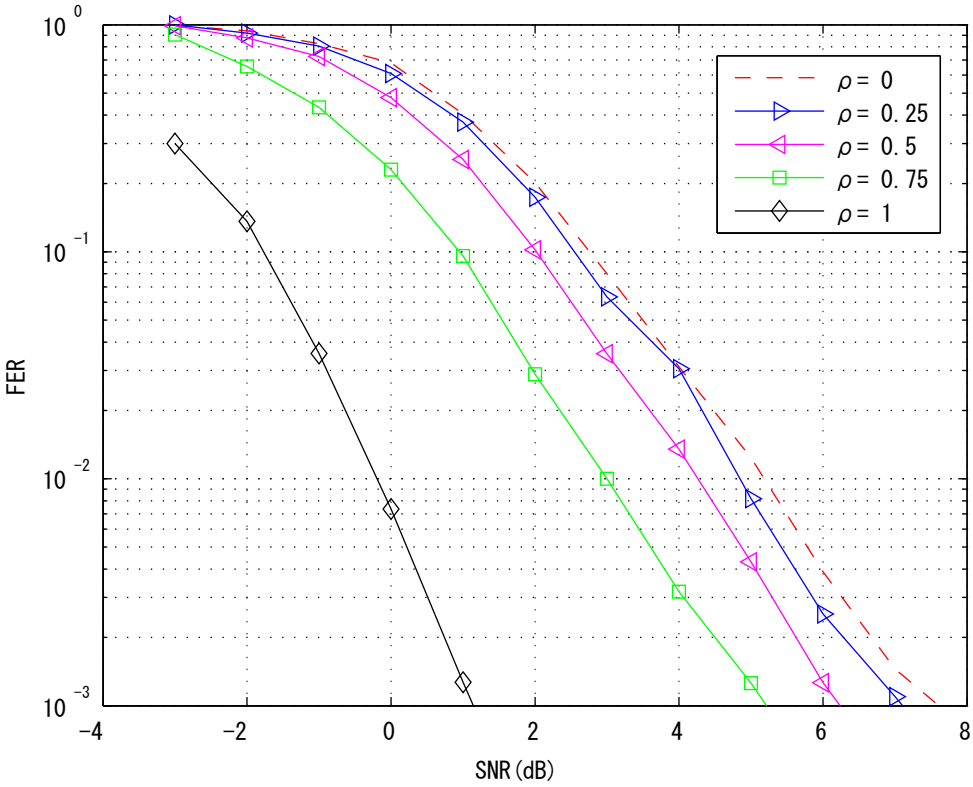

Figure 4.5. FER performance for the 1st user using joint decoder at the receiver

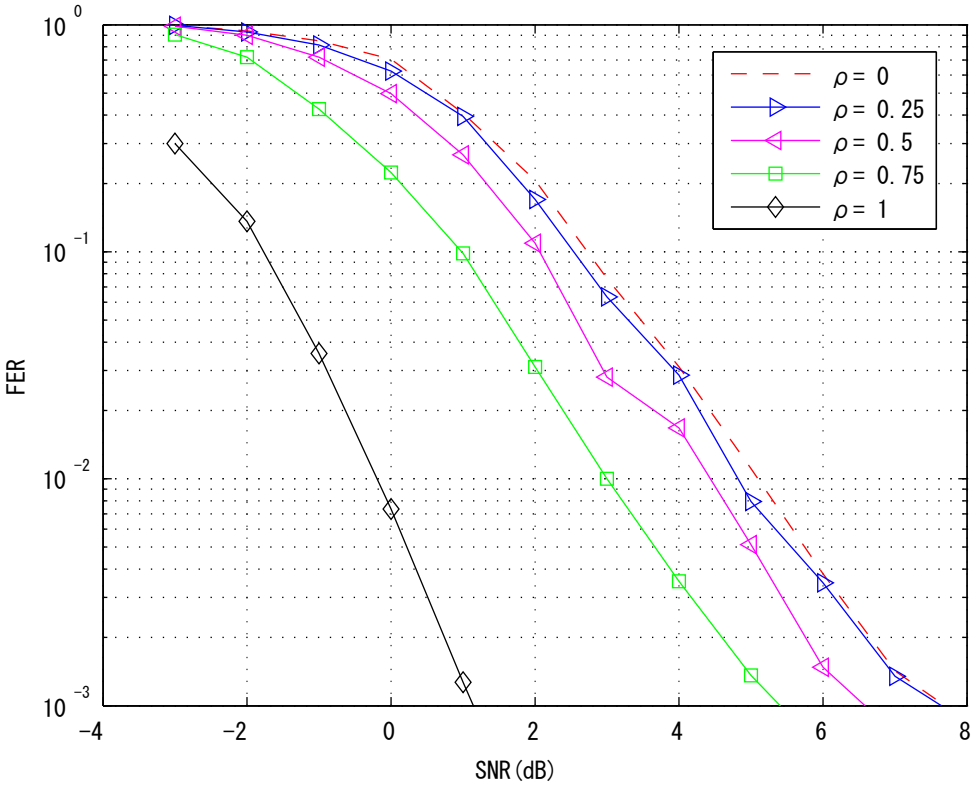

Figure 4.6. FER performance for the 2nd user using joint decoder at the receiver

4.4 Rate-sum / Performance Gain Trade-off

Recall that, in Chapter 2, we have introduced the problem of correlated source transmission over MAC, where Fig. 2.4 shows the rate region with transmission success and fail, based on the sufficient condition proven in [19]. This problem is a combination of Slepian-Wolf rate region and MAC rate region. Since the MAC region with fading channel is not a pentagon, because the MAC region takes the average over the fading variation. Hence, in this section, only AWGN channels are considered. From the computer simulation results provided in the Section 4.3.1, it is obvious that, with higher source correlation, the system can achieve better BER performance, as shown in Fig. 4.3 and Fig. 4.4. However, the total rate of two users is lower while the source correlation is higher. This involves the existence of a trade-off consideration between the rate-sum and the system performance.

This trade-off can be briefly analysed by the interaction part between the S-W region and the MAC region. With a Gaussian codebook, the corner points in the MAC region for the 1st user are defined as:

$$X_1 = C\left(\frac{P_1}{\sigma_n^2}\right) \tag{4.4}$$

$$X_2 = C\left(\frac{P_1}{P_2 + \sigma_n^2}\right), \tag{4.5}$$

which are plotted in Fig. 4.7, with $C(X) = log_2\ (1 + x)$. For the 2nd user, the Equ. (4.4) and (4.5) can be applied for determining the corner points Y_1 and Y_2 as well. In this thesis, per QPSK symbol contains 0.5 information bit. Therefore, it can be known that $E_b/\sigma_n^2 = 2{\cdot}(E_s/\sigma_n^2)$, where E_b and E_s are pre information bit and QPSK symbol energy, respectively. In this section, the definition of SNR should use E_b/σ_n^2. In the Fig. 4.7, we choose the total SNR as $(E_{s1} + E_{s2})/\sigma_n^2 = 0.9103dB$ with unequal power allocation $E_{s1}/E_{s2} = 1.5$, from which E_{s1}/σ_n^2 and E_{s2}/σ_n^2 can be obtained. Then we convert them into E_b/σ_n^2 and calculate corner points of MAC region using Equ. (4.4) and (4.5).

On the other hand, the S-W region in Fig. 4.7 are calculated using Equ. (2.16), with different source correlation ρ. In this thesis, the sources are assumed to be binary and uniformly distributed. Therefore, the entropy of two sources are both equal to 1. The conditional entropy of two sources can be easily calculated by

using the bit-flipping probability p_e as the conditional probability representing the probability of the two sources having different bit, which is defined by $p_e = (1-\rho)/\ 2$.

In the Fig. 4.7, it can be found that with source correlation $\rho = \{0.75,\ 1\}$, the S-W region and MAC region have an intersection area. The corresponding BER values are shown in Fig. 4.3 and Fig. 4.4, which are very low and can be considered as the transmission being successful. However, for the case with source correlation $\rho = \{0,\ 0.25,\ 0.5\}$, the S-W region and MAC region are separated with each other. The corresponding BER values are very high and such situation can be considered as the transmission being failure. Hence, from the observation obtain above, the simulation result are consistent to what we have discussed in Section 2.3 regarding the area overlapping based on the sufficient condition of the problem of correlated sources transmitting over MAC.

Moreover, the rate-sum of different source correlation are calculated by

$$R_1 + R_2 = 1 + h(p_e) \tag{4.6}$$

with

$$h(p_e) = -[p_e \cdot log_2\ p_e + (1-p_e) \cdot log_2\ (1-p_e)], \tag{4.7}$$

which is illustrated by dashed lines in Fig. 4.7. With source correlation $\rho = \{0,\ 0.25, 0.5,\ 0.75,\ 1\}$, the rate-sum is as following:

$$R_1 + R_2 = \{2,\ 1.9544,\ 1.8113,\ 1.5436,\ 1\}. \tag{4.8}$$

The relationship between rate-sum and BER performance we obtained above can be considered as the rate-sum / performance trade-off. Considering the two extreme cases in which $\rho = 0$ and 1, the corresponding rate-sum are 2 and 1, respectively. When $\rho = 0$, two sources are independent, thus, information rate is twice as large as with $\rho = 1$, but with a relatively bad BER performance result. However, when $\rho = 1$, two sources are exactly the same, which is equivalent to that one information is transmitted twice, and hence the BER performance is good with the expected of rate-sum loss. Therefore, the trade-off between rate-sum and performance for the cases of $0 \leq \rho \leq 1$ were demonstrated as shown below for the IDMA-BICM-ID MAC transmission strategy. With certain SNR and power allocation in the AWGN channel, the MAC region is fixed. In this case, better BER

performance can be achieved with less information being transmitted. However, we can also transmit more information if a relatively high BER performance can be accepted. This trade-off is useful in the cooperative communications, where we can optimise the transmission power and rate trade-off for the each user.

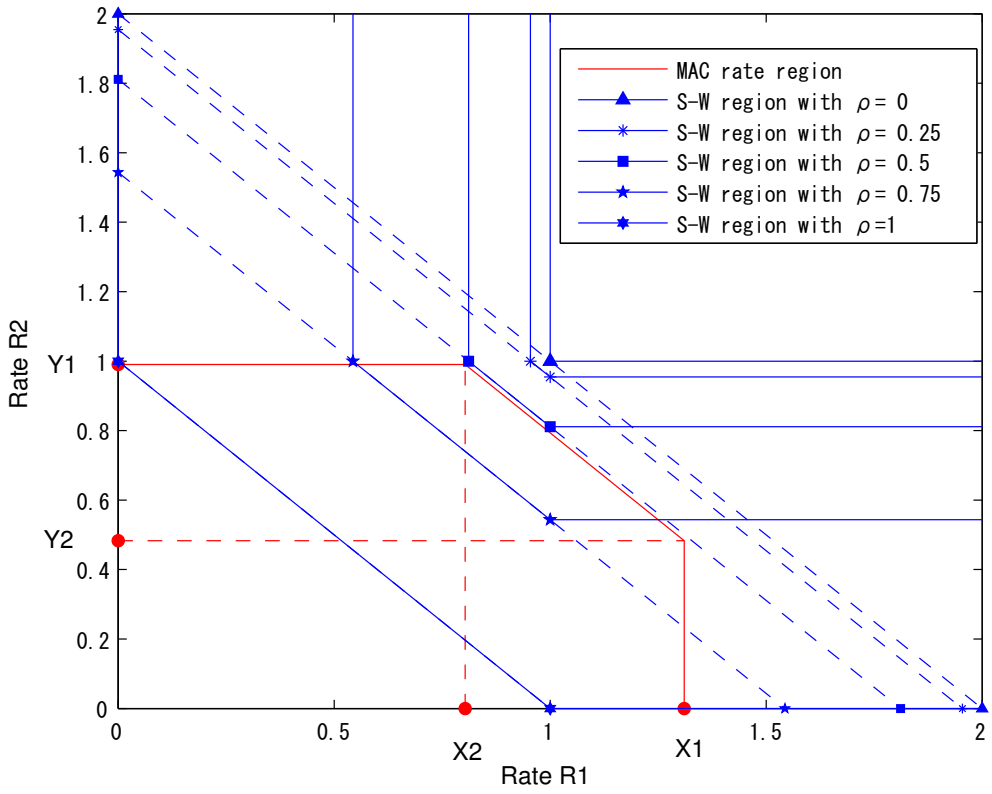

Figure 4.7. Rate-sum/ performance gain trade-off analysis. E_s/σ_n^2 for the 1st user and the 2nd user are $-1.3083dB$ and $-3.0691dB$

4.5 Summary

In this chapter, we have investigated the impact of source correlation on IDMA-based MUD with joint decoder. We first introduced the modified system model, including the principle and properties of joint decoder, and the modified iteration scheme. Then, we provided the numerical results based on the IDMA-based MUD system with joint decoder in AWGN channel and frequency selective fading channel using the same simulation parameters and algorithms as in Chapter 3. After that, the rate-sum / performance gain trade-off was discussed through the S-W and MAC rate region.

From the numerical results, it has been found that, with higher source correlation, system can achieve better BER and/or FER performance in AWGN channel as well as in frequency selective fading channel. Especially, with correlation coefficient $\rho = 1$, it is equivalent to that one information is transmitted twice. Hence, with $\rho = 1$, a large gap between the case whose $\rho < 1$ is observed and can increase the diversity order twice as large as in the frequency selective fading channel with $\rho < 1$.

Moreover, the rate-sum / performance gain trade-off was deep discussed. It is obvious that the MAC region is fixed with certain SNR and physical resources allocation in practical system, such as power or transmission rates. Therefore, there exists a conflict between the transmission efficient and reliability with limited the physical resources. This situation is quite common in the cooperative communications, where, in many cases, we are trying to transmit more information with limited physical resources. By utilizing the trade-off analysis described in this chapter, with certain resources, it is possible to allocate and optimise the powers and/or transmission rates to achieve larger rate-sum or better performance depending on the QoS requirement of applications.

Chapter 5

Conclusions and Future Work

5.1 Conclusions

In this thesis, we have investigated the impact of source correlation on IDMA-based MUD. It has been found that with independent decoding, the source correlation dose not make any impact on system performance at all, due to the interleavers in the IDMA transmitter temporarily removing the source correlation at the transmission symbol-level, where SSIC is performed for MUD. It is then verified that, with the help of joint decoder which aims to utilize the source correlation knowledge, the BER performance in AWGN channel as well as the FER performance in frequency selective fading channel, can be further improved by exchanging correlation knowledge between the decoders. In the frequency selective fading channel, the *joint FD-SC-MMSE equalizer and demapper* is utilized to eliminate ISI due to the multipath propagation. Moreover, an analysis result on rate-sum / performance gain trade-off is also provided to analyse the problem of correlated sources transmitted over MAC through the S-W and MAC rate region analysis.

In Chapter 2, we introduced several basic principles and techniques which are used in this research, including IDMA principle, channel models, the problem of the correlated sources transmitted over MAC and signalling-coding-decoding schemes. In this chapter, we briefly introduced the sufficient condition to achieve arbitrary low BER and/or FER for the problem of correlated sources transmitted over MAC and several related analysis results, which are the base of the trade-off analysis in Chapter 4.

In Chapter 3, we first provided the system model of IDMA-based MUD trans-

mitter and receiver with independent decoding assumed at the receiver side, as well as the structure and algorithm of the *joint FD-SC-MMSE equalizer and demapper* for eliminating the ISI in frequency selective fading channel. In this chapter, the process of SSIC and the iteration schemes were also provided. From the simulation results, the IDMA system can achieve almost the same the BER performance for both two users even with different source correlations which are set as a parameter in the simulations. This is because the interleavers in the IDMA transmitter temporarily removed the source correlation at the symbol-level. The same conclusion can also be drawn in frequency selective fading channel case as well.

In the Chapter 4, the source correlation was utilized at the receiver by exchanging correlation knowledge between the decoders, of which process is called vertical iteration, and the whole decoding structure is referred to as joint decoder. Since source correlation can be utilized in decoding process, the system performance is better if sources have higher correlation. As the EXIT chart analysis which is taking into account the systematic *a priori* LLR modification function, fc function, it has been found that with relatively low source correlation, the joint decoder does not significantly improve the system performance, while with high source correlation, the joint decoder can significantly increase the *extrinsic* information of channel decoders to improve performance. In the frequency selective fading channels, with $0 \leq \rho < 1$, the joint decoding process does not change the diversity order, only a parallel shift of FER curve can be observed. However, with $\rho = 1$, joint decoding process can increase the diversity order twice as large as with $\rho < 1$.

Moreover, with the analysis of rate-sum / performance gain trade-off, it is concluded that if the SNR is fixed, a trade-off between transmission efficiency and reliability exists. This result can help us to flexibly allocate the power and transmission rate in cooperative communication systems depending on the QoS requirement of the applications.

5.2 Future Work

Based on the result obtained in this research, applying the IDMA-based MUD into cooperative communication with more users, and power, rate allocations, are potential and very interesting topics as the future work. In this research, for

simplicity, the number of users is set to 2. However, in practical cooperative communication systems, such V2V network and WSN, there usually exists more than 2 users. Therefore, the transmission scheme, such as power allocation, with more than two users should be investigated. Since through non-orthogonal MAC it is possible to achieve higher transmission efficiency, techniques used in this research can also be exploited into future wireless communications in ubiquitous environments, which might contain some unpredictable properties, such as a fast changing topology or relatively larger source correlation. Outage probability analysis under frequency selective fading MAC is also very important but left unsolved.

Furthermore, the rate region analysis of rate-sum / performance gain trade-off is also a challenging future topic. By utilizing a close-capacity achieving code, we can obtain more accurate intersection analysis results between S-W and MAC rate regions. However, deriving the necessary condition for achieving arbitrary low error rate in the MAC in forms of the S-W and MAC region is still left as an open question in Network Information Theory.

Bibliography

[1] P. Wang, J. Xiao, and L. Ping, "Comparison of orthogonal and nonorthogonal approaches to future wireless cellular systems," *IEEE Vehicular Technology Magazine*, vol. 1, no. 3, pp. 4–11, 2006.

[2] L. Ping, L. Liu, K. Wu, and W. K. Leung, "Interleave division multiple-access," *IEEE Transactions on Wireless Communications*, vol. 5, pp. 938–947, April 2006.

[3] H. Schoeneich and P. A. Hoeher, "Adaptive interleave-division multiple access-a potential air interface for 4g bearer services and wireless lans," in *Proc. WOCN 2004*, pp. 179–182, 2004.

[4] P. A. Hoeher and H. Schoeneich, "Interleave-division multiple access from a multiuser theory point of view," in *Turbo Codes&Related Topics; 6th International ITG-Conference on Source and Channel Coding (TURBOCODING), 2006 4th International Symposium on*, pp. 1–5, VDE, 2006.

[5] C. Berrou, A. Glavieux, and P. Thitimajshima, "Near shannon limit error-correcting coding and decoding," in *IEEE ICC'93*, pp. 1064–1070, 1993.

[6] E. Zehavi, "8-psk trellis codes for a rayleigh channel," *IEEE Transactions on Communications*, vol. 40, no. 5, pp. 873–884, 1992.

[7] L. Hanzo, T. H. Liew, and B. L. Yeap, *Turbo coding, turbo equalisation and space-time coding*. John Wiley & Sons, 2002.

[8] X. Li and J. A. Ritcey, "Bit-interleaved coded modulation with iterative decoding," *IEEE Communications Letters*, vol. 1, no. 6, pp. 169–171, 1997.

[9] K. Fukawa, D. Zhao, A. Tolli, and T. Matsumoto, "Irregular repetition and single parity check coded bicm-id using extended mapping-optimal node degree allocation," in *Communications and Networking in China (CHINACOM), 2010 5th International ICST Conference on*, pp. 1–6, IEEE, 2010.

[10] S. Ormsub, K. Fukawa, A. Tolli, and T. Matsumoto, "Near-capacity-achieving simple bicm-id," in *2011 IEEE Communication Theory Workshop*, 2011.

[11] S. ORMSUB, "Near-capacity-achieving design of bicm-id based idma," 2012.

[12] K. WU, K. Anwar, and T. Matsumoto, "Bicm-id-based idma: Convergence and rate region analyses," *IEICE Transactions on Communications*, vol. 97, no. 7, pp. 1483–1492, 2014.

[13] K. Wu, K. Anwar, and T. Matsumoto, "Joint turbo equalization and bicm-id-based idma over frequency selective fading channels," in *Information Theory and its Applications (ISITA), 2014 International Symposium on*, pp. 502–506, IEEE, 2014.

[14] C. E. Shannon, "A mathematical theory of communication," *Bell System Technical Journal*, vol. 27, pp. 379–423,623–656, 1948.

[15] W. C. Jakes and D. C. Cox, *Microwave mobile communications*. Wiley-IEEE Press, 1994.

[16] A. Goldsmith, *Wireless communications*. Cambridge university press, 2005.

[17] T. M. Cover and J. A. Thomas, *Elements of information theory 2nd Edition*. John Wiley & Sons, 2006.

[18] D. Slepian and J. Wolf, "Noiseless coding of correlated information sources," *IEEE Transactions on information Theory*, vol. 19, no. 4, pp. 471–480, 1973.

[19] T. Cover, A. E. Gamal, and M. Salehi, "Multiple access channels with arbitrarily correlated sources," *IEEE Transactions on Information Theory*, vol. 26, no. 6, pp. 648–657, 1980.

[20] A. El Gamal and Y.-H. Kim, *Network information theory*. Cambridge university press, 2011.

[21] M. Cheng, K. Anwar, and T. Matsumoto, "Outage analysis of correlated source transmission in block rayleigh fading channels," in *Vehicular Technology Conference (VTC Fall), 2012 IEEE*, pp. 1–5, IEEE, 2012.

[22] K. Anwar and T. Matsumoto, "Iterative spatial demapping for two correlated sources with power control over fading mac," in *Vehicular Technology Conference (VTC Spring), 2012 IEEE 75th*, pp. 1–7, IEEE, 2012.

[23] R. Rajesh and V. Sharma, "Transmission of correlated sources over a fading multiple access channel," in *Proceedings of the 46th Annual Allerton Conference, Allerton House, UIUC, IL, USA*, vol. 2326, p. 858864, 2008.

[24] X. Zhou, X. He, M. Juntti, and T. Matsumoto, "Outage probability of correlated binary source transmission over fading multiple access channels," in *2015 IEEE 16th International Workshop on Signal Processing Advances in Wireless Communications (SPAWC)*, pp. 96–100, IEEE, 2015.

[25] K. Anwar and T. Matsumoto, "Spatially concatenated codes with turbo equalization for correlated sources," *IEEE Transactions on Signal Processing*, vol. 60, no. 10, pp. 5572–5577, 2012.

[26] A. Aljohani, Z. Babar, S. X. Ng, and L. Hanzo, "Distributed source–channel coding using reduced-complexity syndrome-based ttcm," *IEEE COMMUNICATIONS LETTERS*, vol. 20, no. 10, p. 2095, 2016.

[27] S. Pfletschinger and F. Sanzi, "Error floor removal for bit-interleaved coded modulation with iterative detection," *IEEE Transactions on Wireless Communications*, vol. 5, no. 11, pp. 3174–3181, 2006.

[28] M. Chen, "Outage analysis and optimal power allocation for distributed coding based wireless cooperative communications," 2014.

[29] S. Ten Brink, "Convergence behavior of iteratively decoded parallel concatenated codes," *IEEE transactions on communications*, vol. 49, no. 10, pp. 1727–1737, 2001.

[30] L. Bahl, J. Cocke, F. Jelinek, and J. Raviv, "Optimal decoding of linear codes for minimizing symbol error rate (corresp.)," *IEEE Transactions on Information Theory*, vol. 20, no. 2, pp. 284–287, 1974.

[31] W. W. Peterson and E. J. Weldon, *Error-correcting codes*. MIT press, 1972.

[32] K. Kansanen and T. Matsumoto, "An analytical method for mmse mimo turbo equalizer exit chart computation," *IEEE Transactions on Wireless Communications*, vol. 6, no. 1, pp. 59–63, 2007.

[33] K. Anwar and T. Matsumoto, "Accumulator-assisted distributed turbo codes for relay systems exploiting source-relay correlation," *IEEE Communications Letters*, vol. 16, no. 7, pp. 1114–1117, 2012.